

# Neodymium Alkoxides: Synthesis, Characterization and Their Combinations with Dialkylmagnesiums as Unique Systems for Polymerization and Block Copolymerization of Ethylene and Methyl Methacrylate

Jérôme Gromada,<sup>[a]</sup> André Mortreux,<sup>[a]</sup> Thomas Chenal,<sup>[a]</sup> Joseph W. Ziller,<sup>[b]</sup> Frédéric Leising,<sup>[c]</sup> and Jean-François Carpentier\*<sup>[d]</sup>

**Abstract:** The synthesis and characterization (NMR and X-ray) of a variety of neodymium alkoxides derived from simple and functionalized tertiary monoalcohols, and their application as inorganic precursors in combination with dialkylmagnesium reagents for ethylene and methyl methacrylate (MMA) (co-)polymerization have been investigated. Salt metathesis reactions between  $\text{NdCl}_3$  and sodium alkoxides in THF led to the formation of trinuclear complexes  $[\text{Nd}_3(\mu_3\text{-OR})_2(\mu_2\text{-OR})_3(\text{OR})_4(\text{thf})_2]$  with  $\text{R} = t\text{Bu}$  (**1**),  $t\text{Am}$  (**2**), while aggregate structure  $[\text{Nd}_{12}(\text{OtAm})_{26}(\text{HOtAm})_2\text{Cl}_{11}\text{-Na}] \cdot (\text{OEt}_2)_2$  (**3**) was obtained when the synthesis was performed in  $\text{Et}_2\text{O}$ .  $[\text{Nd}_3(\mu_3\text{-OtBu})_2(\mu_2\text{-OtBu})_3(\text{OtBu})_4(\text{HOtBu})_2]$  (**4**), prepared by aminolysis of  $\text{Nd}[\text{N}(\text{SiMe}_3)_2]_3$  in hexane, slowly decomposed in toluene into oxo complex

$[\text{Nd}_5(\mu_5\text{-O})(\mu_3\text{-OtBu})_4(\mu_2\text{-OtBu})_4(\text{OtBu})_5]$  (**5**). Finally, the dimer  $[\text{Nd}_2(\mu_2, \eta^2\text{-OR})_2(\eta^2\text{-OR})_2(\eta^1\text{-OR})_2]$  ( $\text{OR} = \text{OCMe}_2\text{CH}_2\text{-CH}_2\text{OMe}$ ) (**6**) was synthesised by aminolysis reaction from the corresponding  $\gamma$ -donor-functionalized alcohol. Some of these neodymium alkoxides, in particular homoleptic complex **1**, when associated in situ to one equivalent of a dialkylmagnesium, allow the formation of an active catalyst for ethylene polymerization. Under mild conditions ( $0^\circ\text{C}$ , 1 bar), the latter catalyst system exhibited a moderate activity ( $5\text{--}10 \text{ kg mol}^{-1} \text{ h}^{-1} \text{ bar}^{-1}$ ). Effective transfer reactions were observed in the presence of  $\text{H}_2$  or  $\text{PhSiH}_3$  and renewal/improve-

ment of activity occurred upon extra addition of dialkylmagnesium. The most outstanding feature of this catalytic system lies in the precipitation of the active “Nd-polyethylenyl” species during the ethylene polymerization course as solid **S** which could be isolated. This heterogeneity was turned to good account, enabling to achieve heterogeneous solid–gas ethylene polymerization and to prepare diblock PE-PMMA copolymers with high diblock efficiency and high molecular weights ( $M_n > 200\,000$ ). A catalytic cycle for this unique system is proposed based on the isolation of a transmetallation product (**7**) from a neodymium alkoxide/dialkylmagnesium combination and NMR studies of the latter.

**Keywords:** lanthanides • magnesium • polymerization

[a] J. Gromada, Prof. A. Mortreux, Dr. T. Chenal  
Laboratoire de Catalyse de Lille  
UPRESA 8010 CNRS-Université de Lille 1  
59652 Villeneuve d’Ascq Cedex (France)

[b] Dr. J. W. Ziller  
Department of Chemistry, University of California  
Irvine, 92697 CA (USA)

[c] Dr. F. Leising  
Rhodia Recherches  
93308 Aubervilliers Cedex (France)

[d] Prof. J.-F. Carpentier  
Laboratoire Organométalliques et Catalyse  
UMR 6509 CNRS-Université de Rennes 1  
35042 Rennes Cedex (France)  
Fax: (+33) 2-23-23-69-39  
E-mail: jean-francois.carpentier@univ-rennes1.fr

## Introduction

Trivalent lanthanide hydride and alkyl complexes stabilized by two cyclopentadienyl-type ligands,  $\text{Cp}_2\text{LnR}$ ,<sup>[1]</sup> have attracted much attention because of their high efficiency in polymerizing ethylene and also polar monomers.<sup>[2]</sup> Because of the permanent search for new-generation polymerization catalysts, there is currently considerable interest in developing related organolanthanide complexes involving ancillary ligands other than the commonly used cyclopentadienyl-type ligands.<sup>[3]</sup> In this respect, hard, electronegative  $\pi$ -donor ligands such as alkoxides/aryloxides are particularly attractive because they offer strong metal–oxygen bonds that are expected to stabilize complexes of these electropositive metals. Also, the great variety of these ligands conveniently obtained from alcohols allows considerable variation in steric and electronic features.<sup>[4]</sup> The efficient use in polymerization

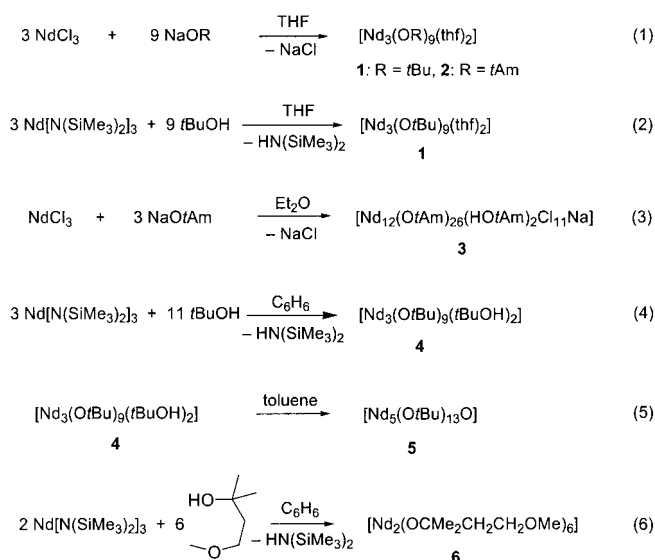
Supporting information for this article is available on the WWW under <http://www.chemeurj.org> or from the author: <sup>1</sup>H NMR spectra of 1:1 mixtures of  $[\text{Nd}_3(\mu_3\text{-OtBu})_2(\mu_2\text{-OtBu})_3(\text{OtBu})_4(\text{thf})_2]$  (**1**)/ $\text{Mg}(n\text{-hex})_2$  and  $[\text{Y}_3(\text{OtBu})_7\text{Cl}_2(\text{thf})_2/\text{Mg}(n\text{-hex})_2]$  (three pages).

of organolanthanide complexes with alkoxide co-ligands was first achieved with the *mixed* Cp-aryloxide system [ $\{Y(C_3Me_5)(O-2,6-tBu_2C_6H_3)(\eta-H)\}_2$ ] that is active for the polymerization of ethylene and higher  $\alpha$ -olefins.<sup>[5]</sup> Recently, other mixed Cp-aryloxide complexes of samarium(II) have been shown to be active for the polymerization and block-copolymerization of ethylene and styrene.<sup>[6]</sup> On the other hand, among the dozen of structurally well-defined cyclopentadienyl-free lanthanide alkyl-alkoxide(aryloxide) complexes that have been reported to this date,<sup>[7–16]</sup> only the neutral dialkyl-aryloxide complex  $[Y\{CH(SiMe_3)_2\}_2(O-2,6-tBu_2C_6H_3)(thf)_2]$  has been shown to exhibit very low ethylene polymerization activity ( $9 \times 10^{-3}$  kg PE mol(Y)<sup>-1</sup> h<sup>-1</sup> bar<sup>-1</sup> at RT).<sup>[9, 18, 19]</sup> This poor ability for ethylene polymerization is rather surprising since alkoxy ligands are expected to render the metal center more electron-deficient and more Lewis acidic.

Further to our work devoted to in situ alkylation of chlorolanthanocene precursors with dialkylmagnesium reagents as alternative, efficient combinations for olefin polymerization,<sup>[20]</sup> we have undertaken a study aimed at replacing chlorolanthanocenes by homoleptic alkoxide lanthanides. Although much data have been collected to date on alkoxide complexes of rare earth elements,<sup>[4]</sup> most of them have focused on yttrium, lanthanum and lutetium because these metals provide diamagnetic compounds characterizable by NMR.<sup>[21–26]</sup> In this study we have chosen to work with neodymium because complexes of this metal have given some of the most active group III metallocene based catalysts for olefin polymerization.<sup>[2]</sup> Considering the complexity of the alkoxy chemistry of lanthanides,<sup>[4]</sup> we felt it was essential to obtain structural information on the alkoxide materials we would use as precursors for polymerization. Hence, in this report we describe first the preparation and the structural investigation of some neodymium complexes having simple and functionalized *tert*-alkoxide ligands.<sup>[23, 27–30]</sup> In a second part we show that some of these compounds act as efficient inorganic pre-catalysts, once combined with dialkylmagnesium compounds, for the controlled polymerization of ethylene and ethylene-methyl methacrylate block copolymerization. Insights into the mechanistic aspects of the formation of active species and polymerization reactions are also given. Part of this work has already been communicated.<sup>[31]</sup>

## Results and Discussion

**Synthesis and structural diversity of neodymium alkoxides:** To explore structural, steric and electronic effects on polymerization catalysis, a set of neodymium alkoxide complexes was prepared. In addition to known mononuclear homoleptic complexes, that is  $[Nd(O-2,6-tBu_2-4-Me-C_6H_3)_3]$ <sup>[32]</sup> and  $[Nd(OCtBu)_3(thf)]$ ,<sup>[27a]</sup> several new complexes were synthesized by varying two parameters which have proven essential in the field:<sup>[4]</sup> i) the nature of the alkoxide ligand and ii) the synthetic route.<sup>[33]</sup> A summary of the chemistry presented in this section is given in Scheme 1.



Scheme 1. Routes to neodymin alkoxides.

**a)  $[Nd_3(\mu_3\text{-OR})_2(\mu_2\text{-OR})_3(\text{OR})_4(\text{thf})_2]$  [ $R = t\text{Bu}$  (**1**),  $t\text{Am}$  (**2**):** The reaction of  $\text{NdCl}_3$  with 3 equiv  $\text{NaO}t\text{Bu}$  in THF at 20 °C for three days gives a single primary product (**1**), that can be routinely isolated in 80–90% yield as a pale blue solid [Scheme 1, Equation (1)]. Compound **1** was also obtained in 90% crude yield by treatment of  $\text{Nd}[\text{N}(\text{SiMe}_3)_2]_3$  with an excess (15 equiv) of *tert*-butyl alcohol in THF at 20 °C for three days [Scheme 1, Equation (1)]. Elemental analysis of the bulk materials was consistent with the composition  $[\text{Nd}_3(\text{O}t\text{Bu})_9(\text{thf})_2]$ . Compound **1** dissolves easily in benzene, toluene and hexane. Rather simple <sup>1</sup>H NMR spectra were expected for **1** because of the single resonance per type of *tert*-butoxide ligand and the splitting of the resonances due to the presence of paramagnetic neodymium metal centers. Variable temperature <sup>1</sup>H NMR spectra in  $[D_8]$ toluene of crude samples obtained by either Equation (1) or (2) were, however, complex with broad resonances. The spectra of samples produced by salt metathesis using  $\text{NaO}t\text{Bu}$  [Eq. (1)] and subsequently recrystallized from toluene proved much more informative, featuring at 5 °C seven well-resolved peaks in the region ranging from  $\delta$  45 to –30 ppm (Figure 1).<sup>[34, 35]</sup> Correlation between chemical shift and coordination mode of the alkoxide groups has been previously noted in yttrium and lanthanum complexes of this type; that is, increased bridging is associated with lower field shifts.<sup>[21, 22, 36]</sup> This could not be applied, however, to determine unambiguously the geometry of **1** in solution, due to the effects of the paramagnetic neodymium centers, and a crystallography study was therefore undertaken.

X-ray quality crystals of **1** were grown at –5 °C from a concentrated toluene solution of a sample prepared from  $\text{NaO}t\text{Bu}$ . Complex **1** is a trimetallic compound in which the three neodymium atoms comprise a triangle with doubly bridging alkoxide groups along the edges of the  $\text{Nd}_3$  triangle and triply bridging groups above and below the  $\text{Nd}_3$  plane (Figure 2). One neodymium atom has two terminal *tert*-butoxy ligands and one terminal *tert*-butoxy ligand and a THF

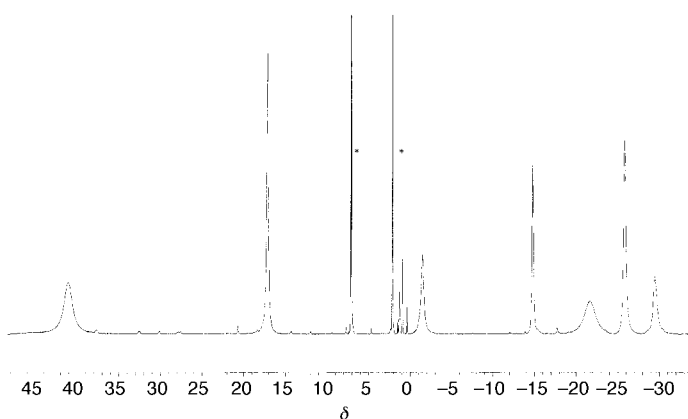


Figure 1.  $^1\text{H}$  NMR spectrum of  $[\text{Nd}_3(\mu_3\text{-OtBu})_2(\mu_2\text{-OtBu})_3(\text{OtBu})_4(\text{thf})_2]$  (**1**) ( $[\text{D}_8]$ toluene,  $5^\circ\text{C}$ ; \* labels indicate residual solvent resonances).

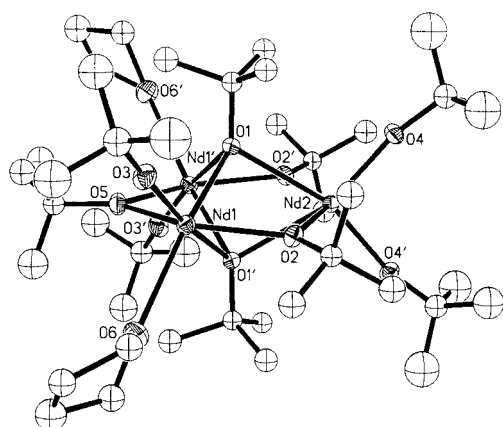


Figure 2. ORTEP plot of  $[\text{Nd}_3(\mu_3\text{-OtBu})_2(\mu_2\text{-OtBu})_3(\text{OtBu})_4(\text{thf})_2]$  (**1**) with probability ellipsoids at 30% (hydrogen atoms omitted for clarity).

molecule ligate each of the two other neodymium atoms. Thus, each neodymium atom in **1** is six-coordinated. The same structure framework has been observed previously in heteroleptic complexes  $[\text{Y}_3(\mu_3\text{-OtBu})(\mu_3\text{-Cl})(\mu_2\text{-OtBu})_3(\text{OtBu})_4(\text{thf})_2]$ <sup>[21a]</sup> and  $[\text{Y}_3(\mu_3\text{-OtBu})(\mu_3\text{-Cl})(\mu_2\text{-OtBu})_3(\text{OtBu})_3\text{Cl}(\text{thf})_2]$ <sup>[21b]</sup> and of homoleptic complex  $[\text{La}_3(\text{OtBu})_9(\text{tBuOH})_2]$ <sup>[23a, 37]</sup> The exact location of the *tert*-butyl alcohol molecules in the latter lanthanum complex could not be formally established because of disorder problems.<sup>[23a]</sup> In both of the aforementioned yttrium complexes, the THF molecules were found to be located on the same side of the  $\text{Y}_3$  plane, as the chloride ligands.<sup>[21a,b]</sup> In contrast, complex **1** has one THF molecule on each side of the trimetallic plane.

Table 1. Selected bond lengths [ $\text{\AA}$ ] and angles [ $^\circ$ ] for complex **1**.

Nd1–O3	2.147(4)	Nd1–O1–C1	123.1(3)
Nd1–O2	2.333(3)	Nd2–O1–C1	120.0(3)
Nd1–O5	2.399(3)	Nd1–O2–C5	131.9(3)
Nd1–O1	2.409(3)	Nd2–O2–C5	126.4(3)
Nd1–O6	2.661(4)	Nd1–O5–C17	130.82(9)
Nd2–O4	2.163(3)	Nd1–O3–C9	177.8(4)
Nd2–O2	2.458(3)	Nd2–O4–C13	167.3(4)
Nd2–O1	2.624(3)	Nd1–O1–Nd1'	94.92(11)
Nd1–Nd1'	3.6318(6)	Nd1–O1–Nd2	95.11(11)
Nd1–Nd2	3.7161(4)	Nd1'–O1–Nd2	92.51(11)
Nd2–Nd1'	3.7161(4)	Nd1–O2–Nd2	101.68(12)

The terminal Nd–O distances of the alkoxide ligands (Nd1–O3 2.147(4), Nd2–O4 2.163(3)  $\text{\AA}$ ) (Table 1) compare well with those found in related complexes, for example  $[\text{Nd}_4(\text{OCH}_2\text{tBu})_{12}]$  (2.138(8)  $\text{\AA}$ ),<sup>[24]</sup>  $[\text{Nd}_2(\text{OCHiPr}_2)_6(\text{L})_2]$  (for L = THF: 2.146(4)–2.160(4)  $\text{\AA}$ , for L = Py: 2.133(4)–2.158(4)  $\text{\AA}$ ),<sup>[29]</sup>  $[\text{Nd}(\text{OCtBu}_3)_3(\text{CH}_3\text{CN})_2]$  (2.149(5)–2.171(5)  $\text{\AA}$ ),<sup>[28a]</sup> and  $[\text{Nd}(\text{OCtBu}_3)_3(\mu\text{-Cl})\text{Li}(\text{thf})_3]$  (2.150(3)–2.171(3)  $\text{\AA}$ ).<sup>[27b]</sup> Doubly bridging Nd–O distances are, as expected, somewhat longer than those of the terminal alkoxide ligands, one  $\mu^2\text{-OtBu}$  ligand forming a symmetric bridge to the two equivalent Nd atoms (Nd1–O5 2.399(3)  $\text{\AA}$ ), while the two other  $\mu^2\text{-OtBu}$  ligands form a disymmetric bridge (Nd1–O2 2.333(3), Nd2–O2 2.458(3)  $\text{\AA}$ ) and average 2.396  $\text{\AA}$ . The latter values are comparable to  $\mu^2$ -bridging Nd–O distances of 2.383(4)–2.394(4)  $\text{\AA}$  found in  $[\text{Nd}_2(\text{OCHiPr}_2)_6(\text{L})_2]$  (L = thf, py, dme),<sup>[29]</sup> and of 2.320(12)–2.381(12)  $\text{\AA}$  in  $[\text{Nd}_4(\text{OCH}_2\text{tBu})_{12}]$ .<sup>[24]</sup> The same comments apply to the triply bridging Nd–O bond length (Nd1–O1 2.409(3), Nd2–O1 2.624(3)  $\text{\AA}$ ). Due to the steric demands in the bridges, all of the three Nd atoms are highly distorted from the ideal octahedral geometry. The Nd1–O3–C9 angle of  $177.8(4)^\circ$  is nearly linear, showing that the thf ligand does not bring significant steric hindrance. On the other hand, because of the replacement of the thf by a terminal bulky OtBu ligand, the Nd2–O4–C13 angle is bent to  $167.3(4)^\circ$ . The elongated Nd1–O6(thf) distance of 2.661(4)  $\text{\AA}$ , compared with the 2.50–2.58  $\text{\AA}$  distances found in  $[\text{NdCl}_3(\text{thf})_4]$ ,<sup>[38]</sup>  $[\text{Nd}_2(\text{OCHiPr}_2)_6(\text{thf})_2]$ ,<sup>[24]</sup>  $[(\eta^5\text{-C}_5\text{H}_5)_3\text{Nd}(\text{thf})]$ ,<sup>[39]</sup> and  $[(\eta\text{-C}_8\text{H}_8)_3\text{Nd}(\text{thf})_2]\{\text{Nd}(\eta\text{-C}_8\text{H}_8)_2\}$ ,<sup>[40]</sup> gives another evidence for steric crowding in this molecule.

Retrospectively, the pattern of seven resonances with an integrated ratio of ca. 2:2:1:1:2:2:1 in the  $^1\text{H}$  NMR spectrum at  $5^\circ\text{C}$  (Figure 1) correlates well with the structure of **1** (Figure 2) which contains nine OtBu groups in five distinct environments and two equivalent thf molecules.<sup>[41]</sup> This suggests that the solid state structure of **1** is retained in hydrocarbon solutions; in particular, this may indicate that there is no transformation at this temperature between the two possible isomers differing in the location of the THF ligands.

The preparation of neodymium *tert*-amyloxide from  $\text{NdCl}_3$  and  $\text{NaOtAm}$  in THF at room temperature was similarly performed, giving a pale-blue solid (**2**) in 66% yield. The variable temperature  $^1\text{H}$  NMR spectra of **2** in  $[\text{D}_8]$ toluene and in  $[\text{D}_8]$ THF are complex. In fact, the expected multiplicity (singlets, triplets, quartets) for the different types of hydrogen was hampered by the paramagnetic neodymium centers and the spectra featured many singlet-like resonances that turned out uninformative. Previous reports have shown that the *tert*-butoxide and the *tert*-amyloxide groups enforce similar structures in group III (Y, La, Pr) alkoxide chemistry.<sup>[23a, 42]</sup> It is therefore reasonable to assume that **2** has the same structure as **1**. This hypothesis is comforted by the nearly identical reactivity of **1** and **2** in ethylene polymerization chemistry (see below).

**b)  $[\text{Nd}_{12}(\text{OtAm})_{26}(\text{HOtAm})_2\text{Cl}_{11}\text{Na}] \cdot (\text{OEt}_2)_2$  (**3**):** When the above salt metathesis reactions between  $\text{NdCl}_3$  and 3 equiv of  $\text{NaOtBu}$  or  $\text{NaOtAm}$  were carried out in diethyl ether instead

of THF as the solvent, the reactions took a different course (Scheme 1, Equation (3)). The crude products recovered after usual workup were slightly soluble in hexane and toluene, and their  $^1\text{H}$  NMR spectra were complex, featuring many resonances with variable line shape. Recrystallization of the crude products from toluene gave crystalline products in low yield in both cases; however, the latter were no longer soluble in toluene nor in THF. X-ray quality crystals were obtained for the *tert*-amylate derivative (**3**) that allowed to establish its geometry in the solid state.

Compound **3** has an unprecedented complex aggregate structure basically formed of four independent trinuclear  $\text{Nd}_3$  units that are linked by sharing  $\mu_2$ -chloro ligands (Figure 3). In

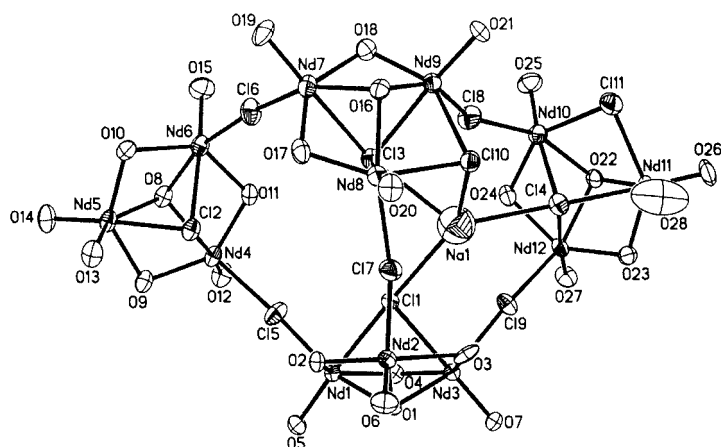


Figure 3. ORTEP plot of  $[\text{Nd}_{12}(\text{OtAm})_{26}(\text{HOtAm})_2\text{Cl}_{11}\text{Na}] \cdot (\text{OEt}_2)_2$  (**3**) with probability ellipsoids at 30% (carbon and hydrogen atoms omitted for clarity).

addition, a sodium atom is present which is coordinated by four chlorine atoms related to three  $\text{Nd}_3$  units and that enforces no symmetry in the molecular structure.<sup>[43]</sup> Schematically, it is possible to divide the structure of **3** in four trimetallic fragments **A–D** and one  $\text{NaCl}$  molecule (Figure 3). The formulas for **A–D**, that do *not* describe the bridging between the fragments, that is  $[\text{Nd}_3(\mu_3\text{-OtAm})(\mu_3\text{-Cl})(\mu_2\text{-OtAm})_3(\text{OtAm})_3\text{Cl}]$  (**A**:  $\text{Nd1–Nd3}$ ),  $[\text{Nd}_3(\mu_3\text{-OtAm})(\mu_3\text{-Cl})(\mu_2\text{-OtAm})_3(\text{OtAm})_3\text{Cl}(\text{HOtAm})]$  (**B**:  $\text{Nd4–Nd6}$ ),  $[\text{Nd}_3(\mu_3\text{-OtAm})(\mu_3\text{-Cl})(\mu_2\text{-OtAm})_3(\mu_2\text{-Cl})(\text{OtAm})_3\text{Cl}]$  (**C**:  $\text{Nd7–Nd9}$ ) and  $[\text{Nd}_3(\mu_3\text{-OtAm})(\mu_3\text{-Cl})(\mu_2\text{-OtAm})_3(\mu_2\text{-Cl})(\text{OtAm})_3\text{Cl}(\text{HOtAm})]$  (**D**:  $\text{Nd10–Nd12}$ ), show structural relationships between these fragments and heteroleptic trinuclear complexes reported in the literature. Thus, fragments **A** and **B** have a formula unit related to  $[\text{Y}_3(\mu_3\text{-OtBu})(\mu_3\text{-Cl})(\mu_2\text{-OtBu})_5(\text{OtBu})_3\text{Cl}(\text{tHF})_2]$ <sup>[21b]</sup> and, structurally, these units are nearly identical. Fragments **C** and **D** feature also a similar structure and a formula unit related to **A** and **B** except that a  $\mu_2\text{-Cl}$  ligand has replaced a  $\mu_2\text{-OtBu}$  ligand. As shown in Table 2, the bond length observed for the terminal alkoxide (2.090(8)–2.113(7) Å in **A** and **B**; 2.070(7)–2.100(7) Å in **C** and **D**), the bridging  $\text{Nd–O}(\mu_2\text{-OR})$  (2.347(7)–2.497(7) Å in **A** and **B**; 2.314(7)–2.380(7) Å in **C** and **D**) and  $\text{Nd–O}(\mu_3\text{-OR})$  (2.442(7)–2.521(6) Å in **A** and **B**; 2.452(7)–2.555(7) Å in **C** and **D**) are similar to those found in **1**. The presence of two coordinated molecules of  $\text{HOtAm}$ , one in fragment **B** and one

Table 2. Selected bond lengths [Å] and angles [°] for complex **3**.

Nd1–O5	2.100(7)	Nd1–O5–C21	163.7(8)
Nd1–O2	2.348(7)	Nd1–O2–C6	127.4(7)
Nd1–O1	2.521(6)	Nd1–O1–C1	118.9(5)
Nd1–Cl5	2.842(3)	Nd1–Cl5–Nd4	169.49(13)
Nd1–Cl1	2.992(2)	Nd1–Cl1–Na1	177.4(2)
Nd2–Cl7	2.834(3)	Nd8–Cl7–Nd2	169.11(12)
Nd2–Cl1	3.009(2)	Nd2–Cl1–Na1	100.1(2)
Nd3–O3	2.483(7)	Nd3–O3–Nd2	98.0(3)
Nd4–Cl5	2.848(3)	O12–Nd4–Cl5	91.9(2)
Nd4–Cl2	3.010(3)	Cl5–Nd4–Cl2	90.87(8)
Nd5–O14	2.109(7)	Nd5–O14–C66	176.7(9)
Nd5–O10	2.374(7)	Nd5–O10–Nd6	103.2(3)
Nd5–O9	2.380(7)	Nd5–O9–Nd4	103.3(3)
Nd5–O8	2.442(7)	Nd5–O8–Nd6	98.2(2)
Nd5–O13	2.545(7)	Nd5–O13–C61	147.0(6)
Nd7–O19	2.090(7)	Nd7–O19–C91	171.1(9)
Nd7–O17	2.370(8)	Nd8–O17–Nd7	105.9(3)
Nd7–O16	2.555(7)	Nd8–O16–Nd7	96.3(2)
Nd7–Cl6	2.792(3)	Nd7–Cl6–Nd6	173.00(14)
Nd7–Cl3	2.991(3)	Nd7–Cl3–Na1	165.2(2)
Nd8–Cl7	2.808(3)	O20–Nd8–Cl7	95.3(2)
Nd8–Cl10	2.870(3)	Nd9–Cl1–Nd8	85.72(7)
Nd8–Cl3	2.945(3)	O20–Nd8–Cl3	173.6(2)
Nd10–Cl4	2.961(3)	Nd10–Cl4–Nd12	77.39(6)
Nd12–Cl9	2.799(3)	Nd12–Cl9–Nd3	170.39(12)

in **D**, is clearly revealed by the longer  $\text{Nd–O}$  bond lengths ( $\text{Nd5–O13}$  2.545(7) Å,  $\text{Nd11–O28}$  2.435(12) Å) compared with the adjacent and other terminal  $\text{Nd–ORAm}$  groups ( $\text{Nd5–O14}$  2.109(7) Å,  $\text{Nd11–O26}$  2.089(8) Å). This is also reflected in the smaller  $\text{La–O–C}$  bond angles ( $\text{Nd5–O13–C61}$  147.0(6)°,  $\text{Nd11–O28–C136}$  158.2(18)°) for the coordinated alcohols, which have only one lone pair for  $\pi$ -donation for donation into vacant metal orbitals, versus the angles of the adjacent covalently bound *tert*-amyloxy groups which have two lone pairs and therefore approach a limiting angle of 180° ( $\text{Nd5–O14–C66}$  176.7(9)°,  $\text{Nd11–O26–C126}$  174.0(10)°). Each of the four  $\text{Nd}_3$  units has one  $\mu_3\text{-Cl}$  ligand with  $\text{Nd–Cl}$  bond lengths in the range of 2.945(3)–3.022(3) Å, values that compare well with that observed in  $[\text{Nd}_6(\text{O}i\text{Pr})_{17}\text{Cl}]$  (3.05(1) Å)<sup>[44]</sup> where the chloride atom is equidistant from the six Nd atoms in a trigonal prism. All fragments **A–D**, as defined with the above formula units, have coordinative vacancies which are filled by linking **A–B**, **B–C**, **C–D**, **D–A** and **A–C** through symmetrically bridging chloride ligands with normal  $\text{Nd}(\mu_3\text{-Cl})$  distances (2.792(3)–2.848(3) Å). The  $\text{Nd–Cl–Nd}$  bond angles for the links between the fragments are all similar (four in the range 169.11(12)–173.00(14)°), except the one linking fragments **C** and **D** (151.97(13)°). This narrow angle likely results from the constraint induced by the coordination of the Na atom. Indeed, the latter is four-coordinated by one  $\mu_3\text{-Cl}$ , two internal  $\mu_2\text{-Cl}$  and one  $\mu_3\text{-Cl}$  bridging two  $\text{Nd}_3$  units, with  $\text{Na–Cl}$  distances in the range of 3.222(11)–3.339(11) Å. These  $\text{Na–Cl}$  distances are much longer than those observed in  $[\text{LnNa}_8(\text{ORBu})_{10}\text{Cl}]$  complexes ( $\text{Ln} = \text{Y, Eu}$ ; 2.642(5)–3.032(5) Å; average  $\text{Na–Cl}$ , 2.82(13) Å).<sup>[43]</sup>

**e**  $[\text{Nd}_3(\mu_3\text{-ORBu})_2(\mu_2\text{-ORBu})_3(\text{ORBu})_4(\text{HOtBu})_2]$  (**4**): The reaction of  $\text{Nd}[\text{N}(\text{SiMe}_3)_2]_3$  with 8 equiv (per mol Nd) of *tert*-butyl alcohol in *n*-hexane at 20 °C gives a single primary

product in 90% yield. Crystallization from toluene yielded violet-blue crystals that analyzed for  $[\text{Nd}_3(\text{OtBu})_9(\text{HOtBu})_2]$  (**4**) (Scheme 1, Equation (4)). Variable temperature  $^1\text{H}$  NMR studies were carried out to derive structural information on this alkoxide in solution. The room temperature 200 MHz  $^1\text{H}$  NMR spectrum of **4** in  $[\text{D}_8]\text{toluene}$  showed very broad resonances characteristic of a fluxional behavior and temperatures below  $5^\circ\text{C}$  were required to slow down the exchange process. Due to effects of the paramagnetic neodymium centers, important variations in the chemical shifts were observed in the temperature range of  $-75$  to  $5^\circ\text{C}$ , causing incidental, potentially misleading, overlapping of some resonances, for example at  $-15$  and  $-65^\circ\text{C}$  (see Experimental Section). The  $^1\text{H}$  NMR spectrum of **4** at  $-45^\circ\text{C}$  showed a major series, accounting for  $96 \pm 2\%$  of total *OtBu* groups, of six well-resolved, relatively sharp resonances with intensities in the ratio 18:36:9:2:18:18, from lower to higher field. This pattern is fully consistent with the trinuclear geometry established for the equivalent yttrium and lanthanum compounds,<sup>[23a]</sup> isostructural to **1**, that contains two capping  $\mu_3$ -*OtBu* groups magnetically equivalent (singlet of relative intensity 2), three bridging  $\mu_2$ -*OtBu* groups in two different environments (2+1), and two terminal ligands for each metal of which two out of six are the coordinated *tBuOH* (2+4). Beside this major set of resonances, a significant minor series of six peaks was also observed in the variable temperature NMR spectra; its relative intensity versus the major series ( $4 \pm 2\%$ ) did not vary within uncertainty in the temperature range of  $-75$  to  $5^\circ\text{C}$ . This suggests, as in the case of **1**, the existence of two isomeric structures differing in the relative location of the coordinated alcohols, that is either both on the same side or on opposite sides of the  $\text{Nd}_3$  plane.

**d)  $[\text{Nd}_5(\mu_5\text{-O})(\mu_3\text{-OtBu})_4(\mu_2\text{-OtBu})_4(\text{OtBu})_5]$  (**5**):** Stirring a toluene solution of complex **4** for two weeks at room temperature resulted in the formation of complex **5** (Scheme 1, Equation (5)). The variable temperature  $^1\text{H}$  NMR spectra in the range of  $-70$  to  $20^\circ\text{C}$  displayed broad, unresolved resonances and did not provide an insight into the solution structure of **5**. The identity of **5** was established by X-ray diffraction (Figure 4, Table 3). The molecular structure corresponds to a pentagonal cluster made of four basal and one apical neodymium centers having each one terminal *OtBu* group, connected by four  $\mu_3$ - and four  $\mu_2$ -bridging *OtBu* groups and comprising a central  $\mu_5$ -oxo ligand. This corresponds to the basic square pyramidal framework observed for lanthanide oxoisopropoxides  $[\text{Ln}_5(\mu_5\text{-O})(\text{O}i\text{Pr})_{13}]$ <sup>[45–47]</sup> and the lanthanum equivalent of **5**, which has been independently reported during the course of this study.<sup>[22b]</sup> The  $\text{Nd}_5$  square pyramid in **5** is quite regular as revealed by the equivalence of the basal Nd atoms and the nearly  $90^\circ$  Nd–O–Nd bond angles (Nd2B–O5–Nd2  $89.60(3)^\circ$ , Nd1–O5–Nd2  $94.8(2)^\circ$ ), with the apical/basal Nd...Nd distance longer than the basal/basal one (3.6550(6) versus 3.5139(5) Å). The Nd–O distances of the terminal alkoxide ligands (Nd1–O1 2.146(9), Nd2–O4 2.138(6) Å), the doubly bridging ligands (Nd2–O3 2.351(3) Å) and the triply bridging ligands (Nd1–O2 2.418(5), Nd2–O2 2.523(3) Å) all fall within the range of values observed for the terminal Nd–O(alkoxy)

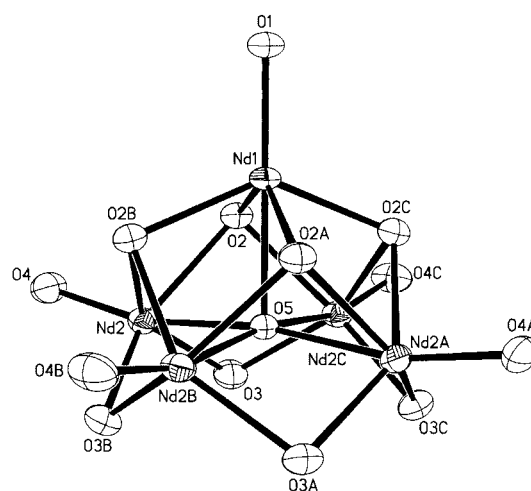


Figure 4. ORTEP plot of  $[\text{Nd}_5(\mu_5\text{-O})(\mu_3\text{-OtBu})_4(\mu_2\text{-OtBu})_4(\text{OtBu})_5]$  (**5**) with probability ellipsoids at 30% (carbon and hydrogen atoms omitted for clarity).

Table 3. Selected bond lengths [Å] and angles [ $^\circ$ ] for complex **5**.

Nd1–O1	2.146(9)	Nd1–O1–C1	180.000(3)
Nd1–O2	2.418(5)	Nd1–O2–C4	126.5(5)
Nd1–O5	2.473(9)	Nd2–O2–C4	121.1(3)
Nd2–O2	2.523(3)	Nd1–O2–Nd2	95.38(15)
Nd2–O3	2.351(3)	Nd2–O3–C7	131.18(12)
Nd2–O4	2.138(6)	Nd2–O3–Nd2C	96.73(18)
Nd2–O5	2.4933(8)	Nd2–O4–C10	178.8(6)
O1–C1	1.402(18)	Nd2–O5–Nd2A	170.4(4)
O2–C4	1.458(10)	Nd1–O5–Nd2	94.8(2)
O3–C7	1.415(13)	Nd2B–O5–Nd2	89.60(3)
O4–C10	1.423(12)	Nd1–O5–Nd2B	94.8(2)

bonds in complexes **1**, **3**, **4**, and the aforementioned neodymium alkoxy complexes. Also, the terminal ligands are associated to nearly linear Nd–O–C angles ( $178.8(6)$ – $180.0(0)^\circ$ ), much larger than those for bridging ligands ( $121.1(3)$ – $131.18(12)^\circ$ ). Contrary to the lanthanum equivalent of **5**,<sup>[22b]</sup> but as observed in  $[\text{Nd}_5(\mu_5\text{-O})(\text{O}i\text{Pr})_{13}]$ ,<sup>[43]</sup> the apical Nd– $\mu_5$ -oxo bond length (Nd1–O5 2.473(9) Å) is only slightly shorter than those involving the basal neodymium centers (Nd2–O5 2.4933(8) Å).

**e)  $[\text{Nd}_2(\mu_2, \eta^2\text{-OR})_2(\eta^2\text{-OR})_2(\eta^1\text{-OR})_2]$  (OR =  $\text{OCMe}_2\text{CH}_2\text{-CH}_2\text{OMe}$ ) (**6**):** The foregoing examples have shown that neodymium centers expand readily their coordination sphere by additional adduct formation despite the presence of the relatively bulky *tert*-butoxy and *tert*-amyloxy ligands. To enforce a lower degree of agglomeration we investigated the use of a  $\gamma$ -donor-functionalized alcohol. The aminolysis reaction of  $\text{Nd}[\text{N}(\text{SiMe}_3)_2]_3$  with three equivalents of the monoclinching alcohol 4-methoxy-2-methylbutan-2-ol in benzene at  $20^\circ\text{C}$  gives, after recrystallization from toluene, blue crystals of **6** [Eq. (6)].<sup>[48]</sup> Again, the variable temperature  $^1\text{H}$  NMR spectra in  $[\text{D}_8]\text{toluene}$  of this compound showed broad, unresolved resonances and proved uninformative with regard to its solution structure.

An X-ray diffraction study revealed that complex **6** adopts in the solid-state a symmetric dinuclear structure in which the ether-alkoxide ligand is found in three different ligation

modes (Figure 5). As shown in Table 4, the neodymium centers are symmetrically bridged by two  $\mu_2, \eta^2$ -ligands through the O(alkoxide) atoms (Nd1–O4 2.3977(12) and 2.3992(12) Å; bite angle O4–Nd1–O3 78.26(4)°). Each neodymium center possesses one terminal  $\eta^2$ -ether-alkoxide ligand (bite angle O2–Nd1–O1 70.70(5)°) and one terminal  $\eta^1$ -alkoxide ligand, and is thus six-coordinated. The axial O1–Nd1–O6 angle of 163.73(5)° is distorted from the idealized 180°, likely because of steric demands in the bridge and in the six-membered chelate ring. This steric crowding is further documented by the bending of the terminal *Ot*Bu ligand (Nd1–O6–C16 163.57(13)°), as discussed for **1**. The Nd–O(alkoxide) bond lengths in **6** lie within the range of values observed for the different structural types of *Ot*Bu ligands in complexes **1**, **3**, **4**, **5** and the other aforementioned neodymium alkoxy complexes. The terminal Nd–O(alkoxide) bond length in the  $\eta^2$ -ligand (Nd1–O2 2.1759(13) Å) is only slightly elongated compared to that in the  $\eta^1$ -ligand (Nd1–O6 2.1526(13) Å); this indicates rather weak ring strain in the terminal  $\eta^2$ -ligand. The Nd–O(ether) contact within this chelate ring (Nd1–O1 2.6629(14) Å) compares well with the long Nd–O(thf) distance of 2.661(4) Å observed in **1**, ascribed to steric crowding. On the other hand, the Nd–O(ether)

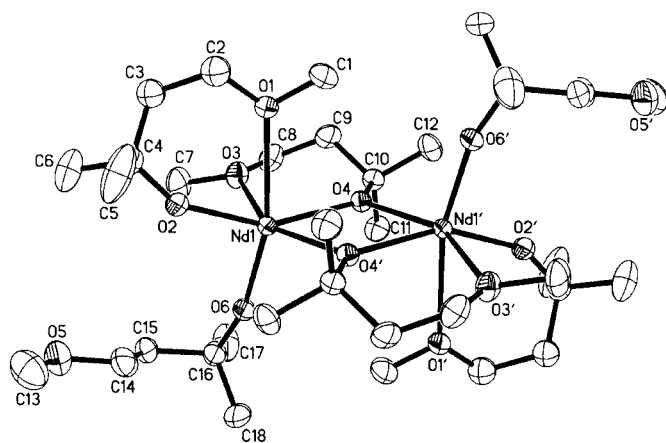


Figure 5. ORTEP plot of  $[\text{Nd}_2(\mu_2, \eta^2\text{-OR})_2(\eta^2\text{-OR})_2(\eta^1\text{-OR})_2]$  (OR = OCMe<sub>2</sub>CH<sub>2</sub>CH<sub>2</sub>OMe) (**6**) with probability ellipsoids at 30% (hydrogen atoms omitted for clarity).

Table 4. Selected bond lengths [Å] and angles [°] for complex **6**.<sup>[a]</sup>

Nd1–O6	2.1526(13)	O4–Nd1–O3	78.26(4)
Nd1–O2	2.1759(13)	O4'–Nd1–O3	150.45(4)
Nd1–O4	2.3977(12)	O2–Nd1–O1	70.70(5)
Nd1–O4'	2.3992(12)	O4–Nd1–O1	84.40(4)
Nd1–O3	2.5198(13)	O4'–Nd1–O1	92.17(5)
Nd1–O1	2.6629(14)	O3–Nd1–O1	79.13(5)
Nd1–Nd1'	3.8615(2)	C1–O1–C2	106.6(2)
		Nd1–O1–C1	119.98(13)
O6–Nd1–O1	163.73(5)	Nd1–O1–C2	126.82(16)
O2–Nd1–O4	154.46(5)	Nd1–O2–C4	151.88(12)
O2–Nd1–O4'	112.67(5)	Nd1–O3–C8	129.22(12)
O6–Nd1–O2	98.62(5)	Nd1–O3–C7	115.49(14)
O6–Nd1–O3	89.12(5)	Nd1–O4–C10	132.30(11)
O6–Nd1–O4	104.34(5)	Nd1'–O4–C10	120.41(10)
O6–Nd1–O4'	103.46(5)	Nd1–O4–Nd1'	107.22(4)
O4–Nd1–O4'	72.78(4)	Nd1–O6–C16	163.57(13)
O2–Nd1–O3	91.21(5)	C13–O5–C14	112.0(2)

[a] Only the major site-occupancy for C2 and C3 are listed.

distance in the  $\mu_2, \eta^2$ -ligand (Nd1–O3 2.5198(13) Å) is comparable to values found in much less crowded complexes, for example  $[\text{NdCl}_3(\text{thf})_3]$  (average 2.50 Å).<sup>[38]</sup>

The solid-state structure of **6** differs significantly from that observed in the homoleptic dinuclear complex  $[\text{Lu}_2(\text{OCMe}_2\text{CH}_2\text{OMe})_6]$ , synthesized according to the silylamide route from the corresponding  $\beta$ -donor-functionalized alcohol.<sup>[25]</sup>  $[\text{Lu}_2(\text{OCMe}_2\text{CH}_2\text{OMe})_6]$  features an asymmetric structure with three  $\mu_2, \eta^2$ -bridging ligands, resulting in a completely different alkoxide environment for the two lutetium centers that are, respectively, six-coordinated and seven-coordinated. Enhanced steric flexibility of our  $\beta$ -functionalized alkoxy ligand and a large difference in the effective ionic radii of the six-coordinated metal centers (Lu<sup>3+</sup> 1.00 Å; Nd<sup>3+</sup> 1.12 Å)<sup>[49]</sup> presumably account for these structural changes.

**f) Comments on synthetic and structural aspects related to neodymium alkoxides:** A set of polynuclear neodymium alkoxides, featuring a remarkable structural diversity and complexity, has been obtained from simple monometallic precursors. Although the detailed intermediates and interconversion processes involved in the construction of these polymetallic alkoxides remain to be clarified, the results described above give clear evidence how specific factors substantially influence the outcome of the syntheses.

Particularly striking is the importance of the reaction details, that is, the choice of alkali metal counteraction and ether solvent, during simple ionic metathesis reactions between NdCl<sub>3</sub> and alkali metal alkoxides. Given the numerous examples in group III organometallic chemistry in which the presence and specific nature of the cation strongly influences the chemistry,<sup>[1, 4]</sup> it is not unreasonable to see somewhat different results in the NaOR versus KOR (R = *t*Bu, *t*Am) reactions.<sup>[35]</sup> Wider variety of products and, in particular, presence of several alkali metal atoms in yttrium alkoxides has been often associated to Li*Ot*Bu (versus Na*Ot*Bu) since lithium appears to be more readily carried along in these systems.<sup>[21]</sup> The incorporation of alkali metal atoms and of chloride in the yttrium systems has been suggested to result from steric considerations;<sup>[21]</sup> contrary to relatively large lanthanides (La<sup>3+</sup> 1.17 Å, Nd<sup>3+</sup> 1.12 Å),<sup>[49]</sup> an yttrium analogue of **1**, that is,  $[\text{Y}_3(\mu_3\text{-OtBu})_2(\mu_2\text{-OtBu})_3(\text{O-}t\text{Bu})_4(\text{thf})_2]$ , would be too crowded because of the two  $\mu_3$ -*Ot*Bu groups, but the small Y<sup>3+</sup> (1.04 Å) would sterically accommodate more easily the less bulky chloride and lithium ions.<sup>[21]</sup> The formation with the early lanthanide Nd<sup>3+</sup> of homoleptic alkoxides **1**, **2** and heteroleptic complex aggregate **3**, upon replacing THF by Et<sub>2</sub>O, respectively, suggests that factors other than steric considerations should be also taken into account. The discrepancy noticed between ethers could be due to the different solubility of metal alkali chlorides and/or LnCl<sub>3</sub> in these solvents. In addition, the ability of LnCl<sub>3</sub> to form THF adducts (LnCl<sub>3</sub>·OEt<sub>2</sub> adducts are not reported in the literature) can also be a likely reason for such differences.

### Olefin polymerization catalysis

As highlighted in the Introduction and will be further illustrated later on in the present study, alkyl/alkoxide meta-

thesis reactions have proved complicated and rather unpredictable. Therefore, a systematic investigation of the reactivity of each lanthanide alkoxide complex we prepared with a variety of potential alkylating reagents would be extremely time- and energy-consuming. In addition, previous work in the field has shown that the isolation of peculiar, structurally well-defined alkyl-alkoxy-lanthanide complexes does not warrant the identification of active olefin polymerization systems (see Introduction). Thus, to explore the ability of the lanthanide alkoxides to serve as Cp-free precursors for olefin polymerization and to detect promising new catalyst systems, we decided to use a more rapid screening approach by investigating directly the reactivity of in situ combinations.

**a) Ethylene polymerization promoted by  $\text{Nd}_x(\text{OR})_y\text{L}_n/\text{MR}_z$  combinations prepared in situ:** A variety of in situ combinations between lanthanide alkoxides and alkylating agents  $\text{MR}_z$ , which may be compared to classic multi-component Ziegler–Natta catalysts, was evaluated in ethylene polymerization by varying both alkyl/alkoxide metathesis (step 1) and polymerization (step 2) conditions, that is,  $\text{Nd}/\text{MR}_z$  ratio, reaction time and temperature, and solvent. The most striking result of this preliminary screening is that only dialkylmagnesium reagents lead to active systems under 1 atm ethylene in toluene; no polymerization activity was detected upon using  $n\text{BuLi}$ ,  $t\text{BuLi}$ ,  $\text{AlMe}_3$ ,  $\text{Al}(n\text{-oct})_3$ ,  $\text{AlH}(i\text{Bu})_2$ ,  $[\text{nBuAlH}(i\text{Bu})_2][\text{Li}]$ ,  $\text{BEt}_3$  or even Grignard reagents ( $\text{PhMgBr}$ ,  $\text{EtMgBr}$ ), under various reaction conditions. It is noteworthy that this does not necessarily imply the absence of alkyl/alkoxide metathesis processes between some of these reagents and the neodymium alkoxides (see below).

Using one equivalent of di(*n*-hexyl)magnesium per mol Nd as co-reagent and toluene or hexane as the solvent, several neodymium alkoxides proved to be effective polymerization catalyst precursors. *tert*-Butoxy- and *tert*-amyloxy neodymium complexes **1** and **2**, prepared by salt metathesis, equally as bulk or recrystallized materials,<sup>[33]</sup> showed a comparable activity, observed since  $-50^\circ\text{C}$  and which proved moderate in the temperature range of  $-20$  to  $40^\circ\text{C}$ . The average activity over 1 h under 1 atm at  $0^\circ\text{C}$  is  $A_{0^\circ\text{C}}$  complex (**1,2**) =  $5\text{--}8 \text{ kg mol}(\text{Nd})^{-1} \text{ h}^{-1} \text{ bar}^{-1}$  (range observed over 10 different experiments and/or batches of **1** or **2**). Activities in the same range were obtained upon using samples of **1** prepared by alcoholysis of the silylamide precursor  $[\text{Nd}(\text{N}(\text{TMS})_2)_3]$  with a slight excess of  $t\text{BuOH}$  in THF [Eq. (2)]; this establishes that possible minor chlorine contamination in samples of **1** prepared by salt metathesis does not interfere to a significant extent. On the other hand, the in situ system based on *tert*-butoxy complex **4**, prepared by a similar alcoholysis route but using benzene as solvent [Eq. (4)] and which is analogous to **1** except that the THF ligands have been replaced by  $t\text{BuOH}$ , showed an activity about two orders of magnitude lower under similar conditions ( $A_{0^\circ\text{C}}$  (complex **4**)  $\approx 0.08 \text{ kg mol}^{-1} \text{ h}^{-1} \text{ bar}^{-1}$ ).<sup>[50]</sup> Homoleptic mononuclear complexes of tritox,  $[\text{Nd}(\text{OC}i\text{Bu}_3)_3(\text{thf})]$ , and of a usual bulky aryloxy ligand,  $[\text{Nd}(\text{O}-2,6\text{-}i\text{Bu}_2\text{-}4\text{-Me-C}_6\text{H}_3)_3]$ , led also to poorly active systems, both requiring temperatures above  $20^\circ\text{C}$  to initiate polymerization ( $A_{40^\circ\text{C}} = 0.6 \text{ kg mol}^{-1} \text{ h}^{-1} \text{ bar}^{-1}$  for both systems).<sup>[50]</sup> Chloro-bridged complex aggregate **3**,

oxo-complex **5** and dinuclear complex **6** with a  $\gamma$ -donor-functionalized alkoxy ligand proved completely ineffective.

It is noteworthy that, although trinuclear complexes **1** and **2** contain two coordinated THF molecules, the addition of 1 mol equiv THF per mol Nd (i.e., 0.3 equiv per mol **1**) proved sufficient to inhibit all polymerization activity.<sup>[51]</sup> Inhibition was also observed when 1 equiv NaCl (or KCl) per mol Nd was added to the  $1/\text{Mg}(n\text{-hex})_2$  (1:1) system. These results show the extreme sensitivity of the active species generated from this combination towards Lewis bases. This may account for the inefficiency of the systems based on Grignard reagents since these potential activators are only available as ether solutions, and those based on complexes **3** and **6**, since they each contain “poisoning” moieties within their structure.<sup>[52]</sup>

**b) Slurry-phase ethylene polymerization promoted by  $1/\text{MgR}_2$  in situ combinations:** In situ combinations of *tert*-butoxy complex **1** and dialkylmagnesium in toluene were selected for further investigations. Representative results are summarized in Table 5 and Figures 6 and 7. In terms of

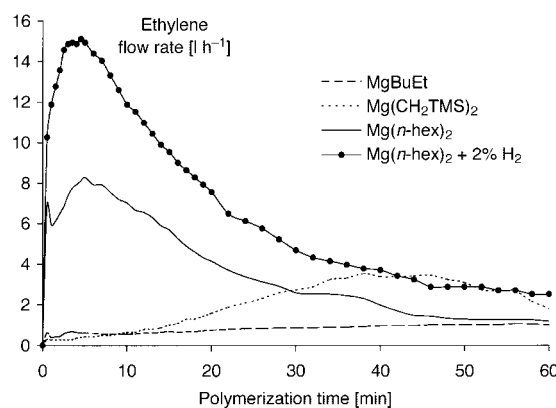


Figure 6. Ethylene flowrates observed with  $1/\text{Mg}(n\text{-hex})_2$  systems ( $\text{Mg}/\text{Nd} = 1.0$ , **1** =  $0.33 \text{ mmol}$ ,  $0^\circ\text{C}$ , 1 atm).

polymerization efficiency, the alkyl/alkoxy metathesis appears to be best conducted at  $0^\circ\text{C}$  for 1 h with different dialkylmagnesium reagents. The nature of the latter affects the activity of the system as judged by the amount of polyethylene recovered after 1 h and also by the ethylene flow rates (Figure 6). Compared to *n*-butylethylmagnesium and di(trimethylsilylmethyl)magnesium, di(*n*-hexyl)magnesium gives the most productive catalyst. The activity of this system hits its maximum after a few minutes and then decreases, concomitantly with the appearance of an insoluble polymer-like material (see below), to reach a plateau, apparently independent of the dialkylmagnesium used (Figure 6). Such a behavior is observed, however, only for a definite Nd to Mg ratio of 1.0, as deviation from this value resulted in a rapid drop of the activity (Figure 7). This contrasts markedly with chlorolanthanocene/dialkylmagnesium systems that proved to accommodate up to 40 equiv  $\text{MgR}_2$  per mol Ln with still high ethylene polymerization activity.<sup>[20]</sup> The activity of the  $1/\text{Mg}(n\text{-hex})_2$  combination at  $0^\circ\text{C}$ , that is,  $A_{0^\circ\text{C}}$  (complex **1**) =  $5\text{--}8 \text{ kg mol}(\text{Nd})^{-1} \text{ h}^{-1} \text{ bar}^{-1}$ ,<sup>[53]</sup> corresponds to a moderate value on absolute Gibson's activity scale,<sup>[17]</sup> which obviously

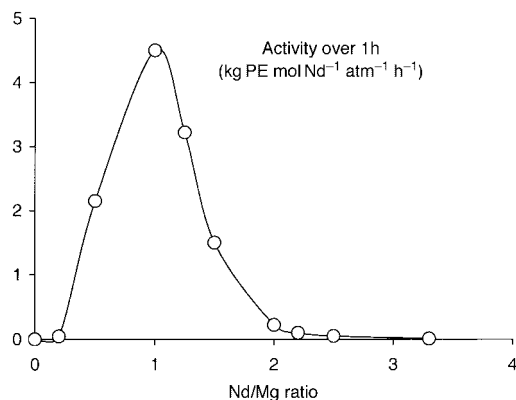


Figure 7. Influence of the Mg/Nd ratio on the polymerization activity of the  $1/\text{Mg}(n\text{-hex})_2$  system ( $1 = 0.33 \text{ mmol}$ ,  $0^\circ\text{C}$ ,  $1 \text{ atm C}_2\text{H}_4$ ).

does not compete with the best multi-component Ziegler–Natta and metallocene catalysts described so far.<sup>[2, 3]</sup> It remains, however, somewhat higher than that for an equivalent lanthanocene system, for example,  $[\text{Cp}^*\text{SmCl}_2\text{Li}(\text{OEt})_2]/n\text{BuEtMg}$  (1:1) gave  $0.34 \text{ kg mol}^{-1}\text{h}^{-1}\text{bar}^{-1}$  under the same reaction conditions.<sup>[20c]</sup>

The polyethylenes recovered under these conditions, after methanol quenching, workup and drying, are highly crystalline (85–90% according to DSC and XRD) with consistent high  $T_m$  in the range  $139\text{--}143^\circ\text{C}$ ,  $M_n = 200\,000\text{--}400\,000$  and  $M_w/M_n = 2.3\text{--}2.5$ . Analysis of aliquots sampled during the polymerization course showed that the polyethylene characteristics do not vary significantly; in particular, high molecular weight polyethylene ( $M_n = 200\,000$ ,  $M_w/M_n = 2.30$ ) is already present after 5 min. The monomodality of the GPC profiles is consistent with the formation of only one type of active species. No low molecular weight chains with vinyl end groups were detected (NMR) in the final polymer produced under these conditions, indicating that at  $0^\circ\text{C}$ ,  $\beta\text{-H}$  elimination and transfer reactions to the monomer are almost absent, if any. Raising the temperature over  $20^\circ\text{C}$  led, however, to a severe decrease in the polymer yield as well as in the molecular weight (e.g., at  $80^\circ\text{C}$ : Table 5, entry 8:  $M_n = 1\,700$ ,  $M_w/M_n = 1.55$ , 29% vinyl chain ends). This is tentatively ascribed to a process involving  $\beta\text{-H}$  elimination and subsequent deactivation of the resulting neodymium-hydride species (see below).

### c) Slurry-phase ethylene polymerizations conducted in the presence of transfer agents: The reactivity of the $1/\text{Mg}(n\text{-hex})_2$

Table 5. Ethylene polymerization using  $1/\text{MgR}_2$  combinations. Influence of reaction conditions on the polymer yield.<sup>[a]</sup>

	MgRR' R, R' =	$T$ alkyl [ $^\circ\text{C}$ ]	$t$ alkyl [min]	$T$ polym [ $^\circ\text{C}$ ]	PE [g]
1	$\text{CH}_2\text{SiMe}_3$	0	60	0	1.80
2	$n\text{Bu, Et}$	0	60	0	1.19
3	$n\text{Bu, Et}$	0	180	0	0.53
4	$n\text{-hex}$	0	60	0	4.70
5	$n\text{-hex}$	0	180	0	1.69
6	$n\text{-hex}$	20	60	0	1.09
7	$n\text{-hex}$	0	60	40	2.75
8	$n\text{-hex}$	0	60	80	0.56

[a] Reactions were carried out in toluene under 1 atm of ethylene for 1 h using 0.33 mmol of **1** and 1.0 mmol of dialkylmagnesium.

combination toward transfer agents was briefly evaluated using phenylsilane and hydrogen. The introduction of 10 equiv  $\text{PhSiH}_3$  (per mol Nd) after 5 min of polymerization did not affect the ethylene flow rate shown in Figure 6 and the related productivity at  $0^\circ\text{C}$ . The analysis of the polymer recovered after 1 h revealed, however, that a transfer reaction had occurred, as the  $M_n$  decreased to 14 300 with  $M_w/M_n = 25$ .  $^1\text{H}$  and  $^{13}\text{C}$  NMR analysis of the polymer clearly showed the formation of end-capped  $\text{PhSiH}_2\text{-polyethylene}$ .<sup>[54]</sup> Dihydrogen proved an even better transfer agent: compared to the reaction carried out with pure ethylene, using 2% (v/v) of  $\text{H}_2$  in ethylene led to a similar activity profile but with almost doubled productivity ( $9\text{--}10 \text{ kg mol}^{-1}\text{h}^{-1}\text{bar}^{-1}$ ) (Figure 6). Analysis of six aliquots sampled every 10 min over the polymerization course under those conditions indicated a constant  $M_n$  value of 17 000 ( $\pm 500$ ) and a molecular weight distribution  $M_w/M_n$  of 5.8, showing that an efficient transfer has also occurred. Effective response of the catalyst system to  $\text{H}_2$  was observed in the range 1–10% (v/v). Nevertheless, this could not be used to prevent catalyst decay at temperatures above  $0^\circ\text{C}$ ; for example, the productivity of the  $1/\text{Mg}(n\text{-hex})_2$  combination at  $20^\circ\text{C}$  in the presence of 2% (v/v) of  $\text{H}_2$  decreased to  $4.4 \text{ kg mol}^{-1}\text{h}^{-1}\text{bar}^{-1}$  ( $M_n = 7\,800$ ;  $M_w/M_n = 37$ ).

**d) Reactivation of in situ systems—Isolation of heterogeneous active polymerization species:** The apparent polymerization activity (ethylene flow rate) of the  $1/\text{Mg}(n\text{-hex})_2$  combination decreases after a few minutes to reach a plateau after 60 min, at  $\approx 1/10$  of the maximal activity (Figure 6). We observed that the latter could be rapidly, although partially restored upon adding 1.0 equiv  $\text{Mg}(n\text{-hex})_2$  per mol Nd to the reaction mixture; then, polymerization proceeded as in the initial batch (Figure 8, straight line). Similar restoration of

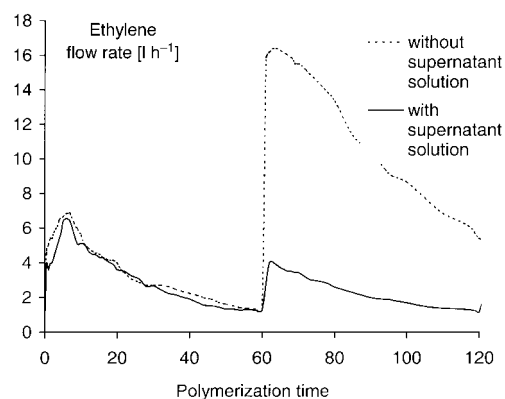


Figure 8. Effect of the addition of 1.0 equiv  $\text{Mg}(n\text{-hex})_2$  (per mol Nd) to the reaction mixtures with (—) and without (•••) supernatant solution on the ethylene flow rates (1.0 mmol Mg and Nd used to prepare the in situ system,  $0^\circ\text{C}$ , 1 atm).

activity was achieved three times consecutively from the same initial in situ combination. This shows that the decrease in the ethylene flow rate does not stem from an irreversible deactivation process but suggests rather a gradual “drowsiness” of the active species, that may be associated to the concomitant accumulation of insoluble, high molecular weight materials over the reaction course.



In order to determine the distribution of total and active Nd in solution (homogeneous) and in the polymeric material precipitated (heterogeneous) during the reaction course, the latter was isolated from the reaction mixture by filtration and subsequently washed with toluene under rigorous exclusion of oxygen and water at 0 °C. The beige solid (**S**) recovered was subjected to microanalyses which revealed, over three different samples, that  $15 \pm 2\%$  of initial Nd (and  $20 \pm 4\%$  of Mg) is present in the precipitate.<sup>[55]</sup> The Nd/Mg ratio in **S**,  $1.2 \pm 0.4$  approaches therefore that introduced for the in situ system (Nd/Mg = 1.0). Most interestingly, when **S** was contacted with ethylene in a fresh toluene slurry (1 atm, 0 °C), polymerization took place with the same activity than in the corresponding in situ experiment, just before its isolation. On the other hand, the clear filtrate that contains  $85 \pm 2\%$  of initial Nd proved completely inactive toward ethylene, even upon reactivation with fresh Mg(*n*-hex)<sub>2</sub>. These results establish that all of the active species generated from the in situ combination of **1** with Mg(*n*-hex)<sub>2</sub> (1:1) are contained in solid **S**. As a matter of fact, it turned out that **S** polymerizes ethylene under solid-gas conditions with significant activity ( $6 \text{ kg mol}^{-1} \text{ h}^{-1} \text{ bar}^{-1}$  over 30 min at 0 °C).

Noteworthy, when a fresh toluene suspension of **S** was treated with 1.0 equiv Mg(*n*-hex)<sub>2</sub> (per mol Nd used in the in situ combination to prepare **S**), the ethylene polymerization activity could be strongly enhanced as compared to the initial polymerization reaction (up to  $100 \text{ kg mol}^{-1} \text{ h}^{-1} \text{ bar}^{-1}$ ) (Figure 8, dotted line). To clarify this phenomenon, which is in direct line with the aforementioned restoration of the catalytic activity upon addition of Mg(*n*-hex)<sub>2</sub> to the in situ system, separate experiments were conducted. No redistribution of Nd metal between the solid and the supernatant toluene solution (ICP elemental analysis) was observed upon treatment of a toluene suspension of **S** with excess of Mg(*n*-hex)<sub>2</sub>. These results rule out the hypothesis of a simple transmetallation process between the dialkylmagnesium reagent and insoluble (slowly active) Nd-polyethylenyl species contained in **S** to form soluble (highly active) Nd-alkyl species. Two other hypotheses that remain to be supported are: i) a scavenging action of MgR<sub>2</sub> comparable to the well-documented effect of trialkylaluminums in group IV-promoted polymerization<sup>[56]</sup> and/or ii) formation of new active sites.

#### e) Ethylene-methyl methacrylate diblock copolymerizations:

A major interest of alkyl-lanthanides in polymerization relies on their unique propensity to induce both polymerization of ethylene and polar monomers.<sup>[2]</sup> We investigated therefore the ability of the new in situ catalyst combination **1**/Mg(*n*-hex)<sub>2</sub> and of isolated compound **S** to initiate the diblock copolymerization of ethylene and methyl methacrylate (MMA). The crude polymer, obtained by initial polymerization of ethylene with the in situ system and subsequent addition of MMA to the reaction mixture at 0 °C, was shown to contain 15–20% of atactic homo-PMMA (Soxhlet extraction with THF for 3 d). This suggests that the in situ combination **1**/Mg(*n*-hex)<sub>2</sub> generates more than one active species for the polymerization of MMA, of which only one is able to initiate the polymerization of ethylene. Indeed, we checked that the solution recovered after filtration of

precipitate **S** from the reaction mixture, that contains 80–85% of Nd and Mg initially introduced but proved inactive towards ethylene, does initiate the polymerization of MMA to give atactic PMMA in moderate activity.<sup>[57]</sup>

On the other hand, the crude polymer recovered from the reaction of MMA with a slurry of solid **S** in fresh toluene at 0 °C contained only 3% of extractable products; <sup>1</sup>H NMR analysis showed that the latter are low molecular weight MMA-rich block copolymers (MMA/ethylene  $\approx$  3). The MMA molar fraction in the THF-insoluble material obtained under typical conditions (see Experimental Section) is  $7 \pm 2\%$  according to the weight increase, <sup>1</sup>H NMR and SEC analyses. The DSC analysis revealed the  $T_g$  of the PMMA block at 122 °C and the  $T_m$  of the PE block as a narrow peak at 142 °C. The SEC analyses of the polyethylene obtained from the hydrolysis of an aliquot of **S** (before addition of MMA) and of the final THF-insoluble material showed an enhancement of the molecular weight from  $M_n = 200\,000$  to  $M_n = 250\,000$  with a  $M_w/M_n$  of 4.0 (monomodal) in both cases. All of these results confirm the true diblock nature of the polymer and, in turn, that ethylene polymerization using the **1**/Mg(*n*-hex)<sub>2</sub> combination proceeds in a “pseudo-living” fashion to give the Nd-polyethylenyl intermediate **S**. In addition to the monomer efficiency of the diblock polymerization process, especially interesting is the possibility to attain block lengths as high as 200 000 for the PE block and  $\approx$  50 000 for the PMMA block. As far as we are aware, these values are significantly higher than those realized with lanthanocene initiators,<sup>[2]</sup> and allow to consider these materials as valuable compatibilizers.<sup>[58]</sup>

#### Mechanistic aspects of Nd<sub>x</sub>(OR)<sub>y</sub>L<sub>n</sub>/MgR<sub>2</sub> systems

The above polymerization results, in particular the effective transfer reactions using PhSiH<sub>3</sub> and H<sub>2</sub> and the possibility to achieve efficient ethylene-MMA block-copolymerization, are in direct line with reactivity trends observed for *alkyllanthanocene* initiators.<sup>[2]</sup> This suggests a polymerization mechanism through coordination–insertion of the monomer onto a alkyl-neodymium species, that would be produced by alkyl/alkoxide metathesis between the alkoxy-lanthanide precursor and the dialkylmagnesium co-reagent. In this section we described our efforts to document this issue.

#### a) Isolation of metathesis products from Nd<sub>x</sub>(OR)<sub>y</sub>L<sub>n</sub>/MR<sub>2</sub> systems:

Repeated attempts to isolate and/or crystallize product(s) formed during the reaction of **1** with dialkylmagnesiums were unsuccessful. Valuable structural information was obtained only with the [Nd(O-2,6-*t*Bu<sub>2</sub>-4-Me-C<sub>6</sub>H<sub>2</sub>)<sub>3</sub>]/Mg(*n*-hex)<sub>2</sub> system; the reaction of these precursors in a 1:1 ratio at room temperature in toluene gives mixed alkyl/aryloxide magnesium compound **7**, which was isolated in 90% yield as colourless crystals and fully characterized by NMR and a X-ray diffraction study (Figure 9).<sup>[59, 60]</sup>

Unfortunately, the neodymium co-product of this metathesis reaction could not be isolated nor identified in solution due to the paramagnetic Nd centers. One may reasonably propose, however, a stoichiometry of the process as outlined in Scheme 2.<sup>[60]</sup> Monitoring the reaction at 20 °C by <sup>1</sup>H NMR showed the gradual formation of uncoordinated 1-hexene (up

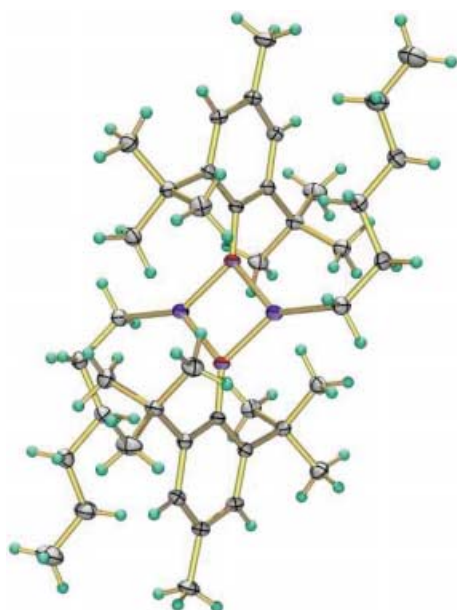
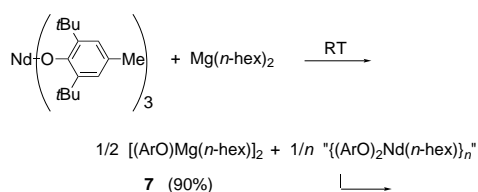


Figure 9. ORTEP plot of  $[(n\text{-hex})\text{Mg}(\text{O}-2,6\text{-}t\text{Bu}_2\text{-4-Me-C}_6\text{H}_2)_2]$  (**7**) with probability ellipsoids at 50%.



Scheme 2. Proposed pathway for the formation of metathesis product **7**.

to 30% per mol Nd after 17 h). Considering the stability of dialkylmagnesium derivatives in general, and of  $\text{Mg}(n\text{-hex})_2$  in particular, towards  $\beta$ -H elimination, this observation suggests that the expected primary product, “ $[(n\text{-hex})\text{Nd}(\text{O}-2,6\text{-}t\text{Bu}_2\text{-4-Me-C}_6\text{H}_2)_2]_n$ ”, is not stable under these conditions and rapidly undergoes  $\beta$ -H elimination to form concomitantly 1-hexene and so far unidentified lanthanide products.

**b) NMR monitoring of  $1/\text{MgR}_2$  combinations:** The reactions of **1** with alkylating reagents were also monitored by variable temperature NMR and led to the following observations, showing similar release of the corresponding  $\alpha$ -olefin. The  $^1\text{H}$  NMR spectrum of a 1:1 mixture of **1** and  $\text{Mg}(n\text{-hex})_2$  in  $[\text{D}_8]$ toluene at  $-80^\circ\text{C}$  showed signals for the unreacted reagents. On raising the temperature, the latter progressively decreased to the profit of at least two sets of resonances attributed to  $t\text{BuO}$  ligands of new neodymium species and the formation of 1-hexene was observed from  $-20^\circ\text{C}$ . No further evolution of the system was noticed after 15 h at  $5^\circ\text{C}$  where 40% of  $\text{Mg}(n\text{-hex})_2$  was transformed into 1-hexene and **1** was completely converted to two new species present in a  $\approx 10:1$  ratio according to  $^1\text{H}$  NMR spectrum. Six resonances in the range of  $\delta = -70$  to 26 ppm with an integrated ratio of 2:1:2:2:1:1 were unambiguously attributed to the major species and suggested a polynuclear structure with  $t\text{BuO}$  ligands in variable (terminal, bridging) environment. Reacting a 1:1 mixture of **1** and  $\text{Mg}(n\text{-hex})_2$  in  $[\text{D}_8]$ toluene directly

at  $20^\circ\text{C}$  for 30 min led to the same mixture of products. When  $n\text{BuMgEt}$  was reacted with **1** under similar conditions, the formation of 1-butene was observed from  $-30^\circ\text{C}$  and reached a maximum of 14% per mol Nd after 15 min at  $20^\circ\text{C}$ . The parallel release of ethylene ( $\delta = 5.26$ ) was detected at temperatures as low as  $-60^\circ\text{C}$  but the amount of this monomer in the reaction medium started to decrease from  $-20^\circ\text{C}$  and no ethylene was detected at  $0^\circ\text{C}$ ; simultaneously, the formation of polyethylene in the NMR tube was observed. This phenomenon is simply rationalized considering the polymerization activity of the  $1/\text{MgR}_2$  systems towards ethylene and its inactivity towards  $\alpha$ -olefins (1-hexene, 1-butene).<sup>[2]</sup> Fast release of 1-butene was also observed from the  $1/n\text{BuLi}$  combination since  $-60^\circ\text{C}$  (up to 20% per mol Nd after 15 min). This suggests rapid alkyl/alkoxy metathesis and subsequent  $\beta$ -H elimination from the resulting  $n\text{Bu}[\text{Nd}]$  species. The high instability of the latter likely accounts for the impossibility to achieve ethylene polymerization from neodymium alkoxide/alkyllithium systems; this also indicates that dialkylmagnesiums may serve not only as alkylating reagents of the alkoxy precursor but also as stabilizers of the resulting alkyl- $[\text{Nd}]$  species, as they do in chlorolanthanocene/ $\text{MgR}_2$  systems through  $\mu$ -alkyl bridging.<sup>[20]</sup> The 1:1 combination of **1** with  $\text{Mg}(\text{CH}_2\text{SiMe}_3)_2$ , an alkylating reagent with no H at the  $\beta$ -position, proved more thermally stable (although not more active for polymerization) but release of isobutene was observed from  $0^\circ\text{C}$  and amounted 40% per mol Nd after 24 h at  $20^\circ\text{C}$ . Some other alkylating reagents lead also to isobutene when combined to **1** but in lower amounts (maximal amount per mol Nd observed after 24 h at  $20^\circ\text{C}$ :  $\text{Mg}(n\text{-hex})_2$ , 4%;  $n\text{BuMgEt}$ , 2%,  $n\text{BuLi}$ , 12%). Formation of isobutene (alkene) has been reported in some cases to occur via simple thermolysis of *tert*-butoxy (alkoxy) lanthanide complexes, without any assistance of alkylating reagent.<sup>[61]</sup> Nonetheless, the smooth conditions under which the release of isobutene proceeds ( $0^\circ\text{C}$ ) and the nearly 1:1 concomitant formation of isobutene and  $\text{SiMe}_4$  (identified by  $^1\text{H}$  and  $^{13}\text{C}$  NMR) upon using  $\text{Mg}(\text{CH}_2\text{SiMe}_3)_2$  suggest that the loss of isobutene proceeds in this case through concerted dealkylation of a  $\text{O}t\text{Bu}$  group by an adjacent alkyl (hydride) group rather than by another  $\text{O}t\text{Bu}$  group. Regardless of the mechanism involved, the expected inorganic co-product is an oxo species, such as for example **5**, but it could not be formally identified so far.

**c) NMR monitoring of diamagnetic  $\text{Ln}_x(\text{OR})_y\text{L}_n/\text{MgR}_2$  systems:** Alkyl derivatives of diamagnetic lanthanide centres can be easily detected by their intrinsic alkyl chemical shifts. Thus, to get additional clues for the probable formation of alkyl-lanthanide species in the systems studied, we have examined metathesis reactions between dialkylmagnesium reagents and  $[\text{La}_3(\text{O}t\text{Bu})_9(\text{thf})_2]$  and  $[\text{Y}_3(\text{O}t\text{Bu})_7\text{Cl}_2(\text{thf})_2]$ . Although combinations of these alkoxides of lanthanum and yttrium with  $\text{Mg}(n\text{-hex})_2$  were found to be significantly less efficient than those based on **1** for ethylene polymerization,<sup>[53]</sup> one might expect from their structural relation to **1** some common reactivity features. In fact, when the reaction of a 1:1 mixture of  $[\text{La}_3(\text{O}t\text{Bu})_9(\text{thf})_2]$  and  $\text{Mg}(n\text{-hex})_2$  in  $[\text{D}_8]$ toluene was monitored by variable temperature  $^1\text{H}$  NMR, a new multiplet

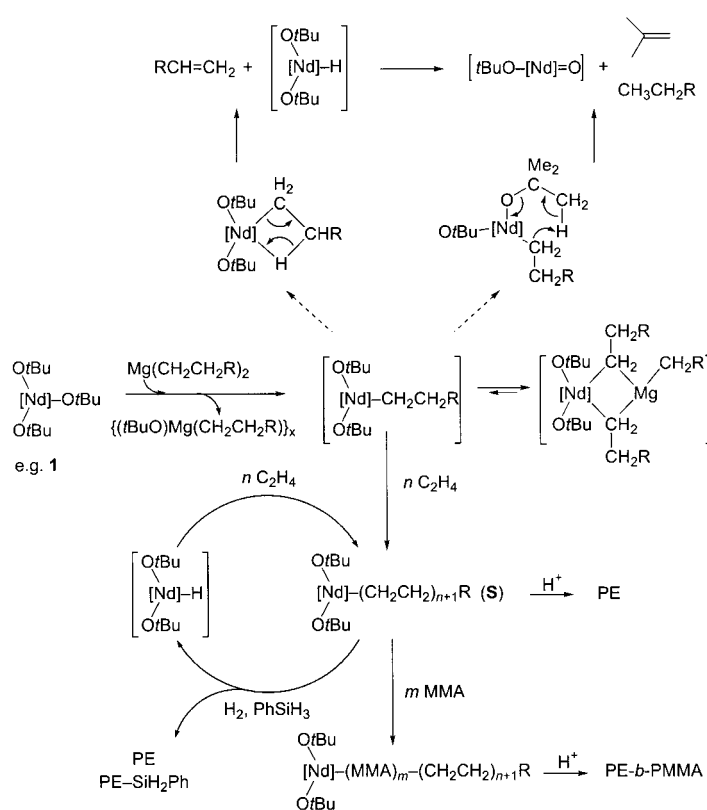
signal at  $\delta = -0.90$  ppm, characteristic of a La-CH<sub>2</sub> moiety,<sup>[16]</sup> appeared from  $-10^\circ\text{C}$  and was observed up to  $20^\circ\text{C}$ . However, its relative intensity remained small with respect to other resonances (*t*BuO, CH<sub>2</sub> from MgR<sub>2</sub>) and the progressive formation of 1-hexene was observed. When the same experiment was carried out using Mg(CH<sub>2</sub>SiMe<sub>3</sub>)<sub>2</sub>, the methylene singlet resonance for this reagent ( $\delta -1.37$ ) disappeared to the benefit of three new singlet resonances in a  $\approx 1:4:2$  ratio ( $\delta = -1.13, -1.23, -1.99$ , respectively). Another informative observation was made upon monitoring the reaction of a 1:1 mixture of [Y<sub>3</sub>(*Ot*Bu)<sub>7</sub>Cl<sub>2</sub>(thf)<sub>2</sub>] and Mg(*n*-hex)<sub>2</sub> in [D<sub>8</sub>]toluene at  $20^\circ\text{C}$ . The <sup>1</sup>H NMR spectra showed the formation of a new multiplet signal at  $\delta = -0.13$  ppm, with couplings of 4 Hz, consistent with <sup>2</sup>J(<sup>89</sup>Y,<sup>1</sup>H) splitting<sup>[7, 9–12]</sup> and products of general formula [Y(*Ot*Bu)<sub>*x*</sub>Cl<sub>*y*</sub>(*n*-hex)<sub>*z*</sub>] were indicated; release of 1-hexene was observed at the same time. These experiments provide therefore clues supporting alkyl/*tert*-butoxide metathetic exchange between lanthanide and magnesium metal centres.<sup>[60]</sup> Not surprisingly in light of previous work in this field,<sup>[7–16]</sup> NMR spectroscopy revealed complex selectivity and stoichiometry of these reactions.

All together these results strongly suggest the formation of one or several [Nd]-{*n*-hex} species from Mg(*n*-hex)<sub>2</sub> and neodymium *tert*-butoxide **1** that show(s) reactivity towards ethylene and some polar monomers similar to that of well-identified alkyl-lanthanocene complexes. A rational representation for the in situ generation of such species, its use as either initiator or catalyst for polymerization and possible decomposition pathways, is proposed in Scheme 3.

## Conclusion

Our results demonstrate that the association of an homoleptic alkoxy neodymium complex with a dialkylmagnesium co-reagent can generate significantly active species for ethylene polymerization. As expected from parallel work in group IV chemistry,<sup>[3]</sup> these Cp-free systems show similar (and sometimes superior) polymerization performance to the corresponding metallocene systems. It confirms thus the ability of some alkoxy/aryloxy residues to act as valuable ancillary ligands for lanthanide metals in the field of polymerization. Several questions arise, however, concerning the difficulties to produce and stabilize such active species. In line with the unsuccessful attempts in this direction,<sup>[7–16]</sup> our results highlight the narrow window in which effective polymerization can be achieved with regards to the nature of the alkoxy-lanthanide precursor and alkylating co-reagent.

In fact, to find an adequate balance between the thermal stability of the alkyl-alkoxy-lanthanide species and their reactivity toward olefin monomers appears as the major issue of this chemistry. NMR investigations indicate a relative easiness of the alkyl/alkoxy metathesis reaction to proceed and the tendency of the resulting alkyl-alkoxy-lanthanide species to undergo rapid  $\beta$ -H elimination and ligand (*tert*-butoxy) thermolysis. In this regard, the exact influence of alkoxy ancillary ligands on the reactivity of alkyl-lanthanide remains a quite controversial issue. On one hand, one may



Scheme 3. Proposed general mechanism for activation and deactivation pathways of *tert*-butoxy-neodymium/dialkylmagnesium polymerization systems.

argue that electron-withdrawing alkoxy ligands, compared to good  $\sigma$ -donor Cp-type ligands, increase the electrophilicity of the metal center and, therefore, facilitate  $\beta$ -H elimination from alkyl-alkoxy-lanthanide species. This simple view may allow for the easy release of  $\alpha$ -olefins observed from combinations of lanthanide alkoxides with alkylating agents in the absence of ethylene. On the other hand, the relative thermodynamics of Ln-C versus Ln-H bond dissociation energies suggests that chain termination ( $\beta$ -H elimination, chain transfer) reactions should be further inhibited or slow, in comparison with the rate of propagation by replacement of Cp\* ligands by hard, electronegative *tert*-butoxide ligands.<sup>[62]</sup> Such arguments have been used to account for the stability of the bridging alkyl groups in [(Y(C<sub>5</sub>Me<sub>5</sub>)(O-2,6-*t*Bu<sub>2</sub>C<sub>6</sub>H<sub>3</sub>)<sub>2</sub>)( $\mu$ -H)( $\mu$ -CH<sub>2</sub>CH<sub>2</sub>R)] toward  $\beta$ -H elimination<sup>[5c]</sup> and fit well with the formation of high molecular weight polymer observed with the [Nd<sub>3</sub>(*Ot*Bu)<sub>9</sub>(thf)<sub>2</sub>]/MgR<sub>2</sub>/ethylene systems.

The high sensitivity of the active species generated from **1**/MgR<sub>2</sub> combinations towards Lewis bases suggests that usual strategies, based on the introduction of additional donor atoms within the ligand framework (e.g. in **6**),<sup>[4d]</sup> may be inappropriate to stabilize alkyl-alkoxy-lanthanide species aimed at ethylene polymerization. We suspect that the adequate (although not ultimate) balance between stability and activity found in **1**/MgR<sub>2</sub> combinations may originate from the degree of aggregation (nuclearity) of the active species and specificities of dialkylmagnesiums (e.g. the electronegativity of Mg which is equivalent to that of the lanthanides).

Formation of dimers and higher polymetallic species has been often related to decreased polymerization activity in group IV chemistry.<sup>[3]</sup> In this regard, it is remarkable that we have detected only sluggish polymerization systems derived from mononuclear lanthanide precursors such as [Nd(O-2,6-*t*Bu<sub>2</sub>-4-Me-C<sub>6</sub>H<sub>2</sub>)<sub>3</sub>] and [Nd(tritox)<sub>3</sub>]. Considering the large bulkiness and robustness of these ligands, one may assume that they induce the formation of monolanthanide alkyl-alkoxy(aryloxy) species.<sup>[7–16]</sup> Much more active polymerization systems derive from trinuclear precursor **1** based on the *tert*-butoxy ligand, which often leads to polynuclear structures due to its relative moderate bulkiness.<sup>[4]</sup> Therefore, it is not unreasonable to think that aggregation to some extent of “[(*t*BuO)<sub>2</sub>LnR]” moieties may contribute to stabilize an active polymerization site. A considerable difficulty usually associated to the chemistry of lanthanide alkoxides relies in their high tendency to form a variety of cluster aggregates, which hampers their isolation in pure form and their characterization. This may prove, however, to be also a key issue for the successful development of new alkoxy-based lanthanide catalysts. Current work is focused on structural investigations of model systems related to these neodymium alkoxide/dialkylmagnesium combinations.

## Experimental Section

**General:** All operations were performed under dry argon using standard Schlenk techniques or in a dry glove box under nitrogen. Solvents and deuterated solvents were freshly distilled from sodium/potassium amalgam under argon and degassed prior to use. Anhydrous NdCl<sub>3</sub> (99.9%) was purchased from Strem and used as received. *tert*-Butyl and *tert*-amyl alcohol were dried over and distilled from CaH<sub>2</sub>. *t*BuONa (97%, Aldrich) and *t*BuOK (95%, Aldrich) were dried at 130 °C under 10<sup>−3</sup> Torr prior to use. Sodium *tert*-amylate was prepared from sodium and *tert*-amyl alcohol at 25 °C; excess alcohol was removed by evaporation and *t*AmONa was dried at 130 °C under high vacuum. Complexes [Nd{N(SiMe<sub>3</sub>)<sub>2</sub>(thf)}<sub>3</sub>]<sup>[63]</sup> [Nd(OC*t*Bu)<sub>3</sub>(thf)]<sup>[27a]</sup> and [Nd(O-2,6-*t*Bu<sub>2</sub>-4-Me-C<sub>6</sub>H<sub>2</sub>)<sub>3</sub>]<sup>[32]</sup> were prepared according to the reported procedures and sublimed prior to use. Ethylene (Air Liquide, N35) was purified by passage through a moisture filter (Chrompack, No. 7971). MMA (99%, Aldrich) was distilled twice over CaH<sub>2</sub> and stored at −20 °C under argon. Alkylating agents AlMe<sub>3</sub>, Al(*n*-oct)<sub>3</sub>, AlH(*i*Bu)<sub>2</sub> (Schering), *n*BuEtMg (20 wt % solution in heptane, Texas Alkyl), Mg(*n*-hex)<sub>2</sub> (1.33 M solution in heptane, Texas Alkyl), PhMgBr (1.0 M solution in THF), EtMgBr (3.0 M solution in THF), BEt<sub>3</sub> (1.0 M solution in hexanes), *n*BuLi (1.6 M solution in hexanes) and *t*BuLi (1.7 M solution in pentane) (all Aldrich) were used as received. Mg(CH<sub>2</sub>SiMe<sub>3</sub>)<sub>2</sub> was prepared according to literature.<sup>[64]</sup> [*n*BuAlH(*i*Bu)<sub>2</sub>][Li] was prepared prior to use from equimolar amounts of AlH(*i*Bu)<sub>2</sub> and *n*BuLi.

NMR spectra of lanthanide alkoxides were recorded on Bruker AC-200, AC-300 or AM-400 spectrometers in Teflon-valved NMR tubes at 23 °C unless otherwise indicated. <sup>1</sup>H (200, 300 and 400 MHz) and <sup>13</sup>C (50, 75 and 100 MHz) chemical shifts are reported versus SiMe<sub>4</sub> and were determined by reference to the residual solvent peaks. Elemental analyses were performed by Pascher Laboratories, Erlangen (Germany) and at Rhodia Research Center, Aubervilliers (France). Molecular weights of polymers were determined by size-exclusion chromatography (SEC) using polystyrene gel columns at 135–155 °C and *ortho*-dichlorobenzene as the solvent, with either a PL220 (Polymer Laboratories) apparatus or a Waters apparatus equipped with coupled refractometer and viscosity detectors. The number-average molecular weight (*M<sub>n</sub>*) and polydispersity ratio (*M<sub>w</sub>*/*M<sub>n</sub>*) were calculated by universal calibration in reference to polystyrene standards. <sup>1</sup>H and <sup>13</sup>C NMR spectra of polymers were recorded on a Bruker AM-400 spectrometer at 130 °C in C<sub>2</sub>D<sub>2</sub>Cl<sub>4</sub>. Melting points (*T<sub>m</sub>*), glass transition temperature (*T<sub>g</sub>*), and crystallinity of polymers were determined by DSC (Setaram DSC 141 apparatus, 10 °C min<sup>−1</sup>, under nitrogen) and

X-ray diffraction (XRD, Siemens D5000 spectrometer, Cu<sub>Kα1,2</sub>, 5° < 2θ < 55°) analysis.

**4-Methoxy-2-methylbutan-2-ol:** A diethyl ether solution of MeMgI (100 mL of a 3.0 M solution, 0.3 mol) in a 250 mL round-bottom flask fitted with an addition funnel under nitrogen was cooled to 0 °C. Methyl 3-methoxypropionate (14.2 g, 0.12 mol) in diethyl ether (90 mL) was added dropwise over 40 min at 0 °C and the reaction mixture was allowed to stir for 18 h at room temperature. The reaction mixture was poured in ice (50 g) and treated with a saturated aqueous solution of NH<sub>4</sub>Cl until clear separation of the two phases occurred. The aqueous layer was extracted with Et<sub>2</sub>O (15 mL). The organic layers were combined, washed first with a cold saturated aqueous solution of NaHCO<sub>3</sub> (30 mL) and then cold water (2 × 30 mL), and dried over MgSO<sub>4</sub>. Removal of the solvent and distillation of the residue (Eb = 85 °C under 95 Torr) gave a colorless liquid (8.4 g, 59%). <sup>1</sup>H NMR (300 MHz, CDCl<sub>3</sub>): δ = 1.21 (s, 6H; CH<sub>3</sub>), 1.73 (t, *J* = 5.9 Hz, 2H; CH<sub>2</sub>), 3.17 (s, 1H; OH), 3.33 (s, 3H; OCH<sub>3</sub>), 3.60 (t, *J* = 5.9 Hz, 2H; OCH<sub>2</sub>); <sup>13</sup>C NMR (75 MHz, CDCl<sub>3</sub>): δ = 29.3 (CMe<sub>2</sub>), 41.4 (CH<sub>2</sub>), 58.9 (MeO), 70.2 (OCH<sub>2</sub>), 70.8 (COH).

### [Nd<sub>3</sub>(μ<sub>3</sub>-*Ot*Bu)<sub>2</sub>(μ<sub>2</sub>-*Ot*Bu)<sub>3</sub>(*Ot*Bu)<sub>4</sub>(thf)<sub>2</sub>] (**1**)

**Salt metathesis route:** In the glovebox, *t*BuONa (2.88 g, 30.0 mmol) was dissolved in THF (50 mL) and transferred to a flask containing a suspension of NdCl<sub>3</sub> (2.51 g, 10.0 mmol) in THF (50 mL). The mixture was stirred with a magnetic stir bar for 3 d at 25 °C. The solution was decanted overnight and filtered, leaving behind a pasty solid that was discarded. Removal of solvents from the solution at 20 °C and drying the residue under 10<sup>−3</sup> Torr for 6 h offered a pale blue solid (3.36 g, 82%). <sup>1</sup>H NMR (400 MHz, [D<sub>8</sub>]toluene): δ (5 °C) = 41.0 (s, 18H), 17.2 (s, 18H), −1.5 (s, 9H), −14.7 (s, 9H), −21.7 (s, 18H), −25.8 (s, 18H), −29.5 (s, 9H); δ (27 °C) = 34.2 (brs, 18H), 14.8 (brs, 18H), −0.5 (brs, 9H), −9.9 (s, 9H), −20.2 (brs, 27H), −22.8 (s, 18H); elemental analysis calcd (%) for C<sub>44</sub>H<sub>97</sub>Nd<sub>3</sub>O<sub>11</sub> (**1**) (1234.97): C 42.79, H 7.92; found: C 41.32, H 7.74; crude samples of **1** prepared by salt metathesis and worked-up as described above were shown to contain less than 0.5% of Cl.

**Amide alcoholysis route:** In a Schlenk tube, *t*BuOH (3.0 mL, 31 mmol) was added dropwise to a stirred solution of Nd[N(SiMe<sub>3</sub>)<sub>2</sub>]<sub>3</sub> (1.25 g, 2.0 mmol) in THF (20 mL). The resulting clear light-blue solution was stirred for 3 d at room temperature. Removal of volatiles under high vacuum for 10 h at room temperature gave a light-blue solid that was subsequently recrystallized from toluene (0.48 g, 57%). The <sup>1</sup>H NMR spectra ([D<sub>8</sub>]toluene, 5 °C) of the crystals featured reproducibly as the major (ca. 70%) peaks the seven resonances observed for samples of **1** prepared from Na*Ot*Bu along with additional (ca. 30%) rather broad resonances at δ = 46.8, 45.5, 40.0, 22.3, 15.1, −27.3, −33.0, −34.1, −42.6.

**X-ray crystal structure determination of 1·THF:** Crystals of **1**·THF were grown from a concentrated toluene solution of the crude product obtained from *t*BuONa at −5 °C. A pale blue crystal of approximate dimensions 0.19 × 0.20 × 0.21 mm was mounted on a glass fiber. X-ray measurements were made using a Bruker SMART CCD area-detector diffractometer with MoK<sub>α</sub> (λ = 0.71073 Å) at *T* = 158(2) K.

Crystal data:<sup>[65]</sup> orthorhombic *Pbcn*: *a* = 17.0538(10), *b* = 20.0343(12), *c* = 17.7400(11) Å; *V* = 6061.1(6) Å<sup>3</sup>; formula unit: C<sub>44</sub>H<sub>97</sub>O<sub>11</sub>Nd<sub>3</sub>·C<sub>4</sub>H<sub>8</sub>O with *Z* = 4; *F<sub>w</sub>*: 1307.04; ρ<sub>calcd</sub> = 1.432 g cm<sup>−3</sup>; *F*(000) = 2676; μ(MoK<sub>α</sub>) = 2.581 mm<sup>−1</sup>. 38059 reflections were collected (1.57° > θ > 28.27°). The structure was solved by direct methods.<sup>[66]</sup> The *tert*-butoxide ligand located on the two-fold axis and the thf ligands were disordered. The carbon atoms associated with these ligands were included using multiple components with partial site-occupancy-factors. There was also one disordered THF solvent molecule present per formula unit. Hydrogen atoms associated with the disordered *tert*-butoxide ligand and with the solvent molecule were not included in the refinement. Full-matrix least-squares refinement on *F*<sup>2</sup> based on 7315 independent reflections converged with 213 variable parameters and 30 restraints. *R*1 = 0.0410 (for those 5589 data with *I* > 2σ(*I*)); *wR*2 = 0.1044; GoF (*F*<sup>2</sup>) = 1.059.<sup>[67]</sup> Δρ<sub>max</sub> = 1.505 and −1.027 e Å<sup>−3</sup>.

**[Nd<sub>3</sub>(μ<sub>3</sub>-*Ot*Am)<sub>2</sub>(μ<sub>2</sub>-*Ot*Am)<sub>3</sub>(*Ot*Am)<sub>4</sub>(thf)<sub>2</sub>] (**2**):** Compound **2** was prepared by salt metathesis similar to **1**, starting from NdCl<sub>3</sub> (2.51 g, 10.0 mmol) and *t*AmONa (3.31 g, 30.0 mmol) in THF (100 mL). Workup left compound **2** as a pale blue solid (3.1 g, 66%). This crude material was directly used for polymerization experiments.

**[Nd<sub>2</sub>(*Ot*Am)<sub>26</sub>Cl<sub>11</sub>Na]·2(Et<sub>2</sub>O) (3·2Et<sub>2</sub>O):** In a glovebox, *t*AmONa (1.67 g, 15.1 mmol) was dissolved in Et<sub>2</sub>O (25 mL) and transferred to a

flask containing a suspension of  $\text{NdCl}_3$  (1.25 g, 5.0 mmol) in  $\text{Et}_2\text{O}$  (25 mL). The mixture was stirred with a magnetic stir bar for 3 d at 25 °C. The solution was decanted overnight and filtered, leaving behind a pasty solid which was discarded. Removal of solvents from the solution at 20 °C and drying the residue under  $10^{-3}$  Torr for 6 h left a blue solid (1.52 g). X-ray quality crystals of **3** were isolated in low yield from a concentrated solution of this material in toluene at –5 °C. The crystals, once isolated, were insoluble even in THF.

**X-ray crystal structure determination of 3·2Et<sub>2</sub>O:** A pale blue crystal of approximate dimensions 0.40 × 0.42 × 0.51 mm was mounted on a glass fiber. X-ray measurements were made using a Bruker SMART CCD area-detector diffractometer with  $\text{MoK}\alpha$  ( $\lambda = 0.71073$  Å) at  $T = 163(2)$  K.

Crystal data:<sup>[65]</sup> monoclinic  $P2_1/c$ :  $a = 30.7931(14)$ ,  $b = 19.9495(9)$ ,  $c = 34.4764(15)$  Å,  $\beta = 105.3890(10)^\circ$ ;  $V = 20419.7(16)$  Å<sup>3</sup>; formula unit:  $\text{C}_{140}\text{H}_{310}\text{Cl}_{11}\text{NaNd}_{12}\text{O}_{28} \cdot 2(\text{C}_4\text{H}_{10}\text{O})$  with  $Z = 4$ ; formula weight: 4733.94;  $\rho_{\text{calcd}} = 1.540$  g cm<sup>-3</sup>;  $F(000) = 9504$ ;  $\mu(\text{MoK}\alpha) = 3.190$  mm<sup>-1</sup>. 153 104 reflections were collected ( $0.69^\circ > \theta > 23.26^\circ$ ). The structure was solved by direct methods.<sup>[66]</sup> There were two molecules of diethyl ether solvent present per formula unit. Two of the *tert*-butoxide ligands were disordered. It was necessary to employ geometric and thermal parameter restraints (2815 total) to all carbon atoms and the solvent molecules via the SHELXTL using the SAME, EADP and PART commands. Disordered atoms were included using multiple components with partial site-occupancy-factors. Hydrogen atoms were not included in the refinement. Full-matrix least-squares refinement on  $F^2$  based on 29327 independent reflections converged with 959 variable parameters and 2815 restraints.  $R1 = 0.0544$  (for those 24067 data with  $I > 2\sigma(I)$ );  $wR2 = 0.1645$ ; GoF ( $F^2$ ) = 1.053.<sup>[67]</sup>  $\Delta\rho_{\text{max}} = 2.469$  and  $-2.199$  e Å<sup>-3</sup>.

**[Nd<sub>3</sub>(μ<sub>3</sub>-OrBu)<sub>2</sub>(μ<sub>2</sub>-OrBu)<sub>3</sub>(OrBu)<sub>4</sub>(HOtBu)<sub>2</sub>] (4):** In a Schlenk tube, *t*BuOH (7.0 mL, 73.0 mmol) was slowly added over ca. 5 min to a stirred solution of  $\text{Nd}[\text{N}(\text{SiMe}_3)_2]_3$  (3.85 g, 6.15 mmol) in *n*-hexane (60 mL). The resulting clear light-blue solution was stirred for 3 d at room temperature. Volatiles were then removed by evaporation in vacuum for 12 h at room temperature to give a light blue solid (2.30 g, 90% based on Nd). Crystallization from toluene offered analytically pure blue crystals (1.55 g, 61%). <sup>1</sup>H NMR (200 MHz, [D<sub>8</sub>]toluene, –15 °C):  $\delta = 19.5$  (s, 18H), 6.4 (s, 45H), –13.5 (s, 2H; OH), –25.2 (s, 18H), –32.0 (s, 18H); (–45 °C):  $\delta = 23.8$  (s, 18H), 9.0 (s, 36H), 5.5 (s, 9H; 1-μ<sub>2</sub>-OrBu), –4.3 (s, 2H; OH), –34.2 (s, 18H), –38.1 (s, 18H); (–65 °C):  $\delta = 27.3$  (s, 18H), 10.9 (s, 36H), 2.7 (s, 9H; 1-μ<sub>2</sub>-OrBu), –6.0 (s, 2H; OH), –42.4 (s, 36H); elemental analysis calcd (%) for  $\text{C}_{44}\text{H}_{101}\text{Nd}_3\text{O}_{11}$  (1239.00): C 42.65, H 8.22; found: C 41.8, H 7.92.

**[Nd<sub>3</sub>(μ<sub>5</sub>-O)(μ<sub>3</sub>-OrBu)<sub>4</sub>(μ<sub>2</sub>-OrBu)<sub>4</sub>(OrBu)<sub>3</sub>] (5):** In a glovebox, **4** (0.720 g, 1.74 mmol Nd) was dissolved in toluene (ca. 5 mL) and the clear blue solution was allowed to stand at room temperature for two weeks. After concentration to ca. 2 mL under vacuum, the solution was placed at –5 °C, leaving X-ray quality crystals of **5**·2(toluene) (which loses toluene in vacuo) (0.310 g, 53%). Elemental analysis calcd (%) for the toluene-free complex  $\text{C}_{52}\text{H}_{117}\text{Nd}_3\text{O}_{14}$  (1687.7): C 37.00, H 6.99; found: C 36.2, H 7.56.

**X-ray crystal structure determination of 5·2(toluene):** A pale purple crystal of approximate dimensions 0.33 × 0.41 × 0.52 mm was mounted on a glass fiber. X-ray measurements were made using a Bruker SMART CCD area-detector diffractometer with  $\text{MoK}\alpha$  ( $\lambda = 0.71073$  Å) at  $T = 163(2)$  K.

Crystal data:<sup>[65]</sup> tetragonal  $P4/nmm$ :  $a = 16.6902(6)$ ,  $b = 16.6902(6)$ ,  $c = 14.0266(7)$  Å;  $V = 3907.3(3)$  Å<sup>3</sup>; formula unit:  $\text{C}_{52}\text{H}_{117}\text{Nd}_3\text{O}_{14} \cdot 2(\text{C}_7\text{H}_8)$  with  $Z = 2$ ; formula weight: 1871.92;  $\rho_{\text{calcd}} = 1.591$  g cm<sup>-3</sup>;  $F(000) = 1882$ ;  $\mu(\text{MoK}\alpha) = 3.317$  mm<sup>-1</sup>. 40 230 reflections were collected ( $1.45^\circ > \theta > 28.29^\circ$ ). The structure was solved by direct methods.<sup>[66]</sup> There were two molecules of toluene solvent present per formula unit. Two of the *tert*-butoxide ligands were disordered. Carbon atoms C2, C3, C11, C12 and C13 were included using partial site-occupancy-factors. The toluene methyl carbon C17 was also disordered and included as above. Hydrogen atoms were not included in the refinement. Full-matrix least-squares refinement on  $F^2$  based on 2710 independent reflections converged with 90 variable parameters and no restraints.  $R1 = 0.0452$  (for those 2410 data with  $I > 2\sigma(I)$ );  $wR2 = 0.1266$ ; GoF ( $F^2$ ) = 1.086.<sup>[67]</sup>  $\Delta\rho_{\text{max}} = 2.561$  and  $-1.211$  e Å<sup>-3</sup>.

**[Nd<sub>2</sub>(OCMe<sub>2</sub>CH<sub>2</sub>CH<sub>2</sub>OMe)<sub>4</sub>] (6):** In a Schlenk tube, 4-methoxy-2-methylbutan-2-ol (0.718 g, 6.06 mmol) dissolved in benzene (10 mL) was added dropwise via canula to a stirred solution of  $\text{Nd}[\text{N}(\text{SiMe}_3)_2]_3$  (1.266 g, 2.02 mmol) in benzene (10 mL). The resulting clear light-blue solution was

stirred for 36 h at room temperature. Evaporation of volatiles, followed by drying under high vacuum for 6 h at 50 °C, gave a blue pasty solid in quantitative yield. Crystallization from toluene at –5 °C offered pure blue crystals suitable for X-ray diffraction (0.58 g, 58%). Elemental analysis calcd (%) for  $\text{C}_{36}\text{H}_{78}\text{Nd}_2\text{O}_{12}$  (991.46): C 43.61, H 7.93; found: C 43.2, H 7.81.

**X-ray crystal structure determination of 6:** A pale purple crystal of approximate dimensions 0.28 × 0.48 × 0.48 mm was mounted on a glass fiber. X-ray measurements were made using a Bruker SMART CCD area-detector diffractometer with  $\text{MoK}\alpha$  ( $\lambda = 0.71073$  Å) at  $T = 163(2)$  K.

Crystal data:<sup>[65]</sup> triclinic  $P\bar{1}$ :  $a = 9.4496(3)$ ,  $b = 10.7702(4)$ ,  $c = 12.8522(5)$  Å;  $\alpha = 96.7120(10)$ ,  $\beta = 96.5560(10)$ ,  $\gamma = 115.7290(10)^\circ$ ;  $V = 1150.21(7)$  Å<sup>3</sup>; formula unit:  $\text{C}_{36}\text{H}_{78}\text{Nd}_2\text{O}_{12}$  with  $Z = 1$ ; formula weight: 991.46;  $\rho_{\text{calcd}} = 1.431$  g cm<sup>-3</sup>;  $F(000) = 510$ ;  $\mu(\text{MoK}\alpha) = 2.282$  mm<sup>-1</sup>. 12 462 reflections were collected ( $1.62^\circ > \theta > 28.30^\circ$ ). The structure was solved by direct methods.<sup>[66]</sup> Carbon atoms C2 and C3 were disordered and included using multiple components with partial site-occupancy-factors (major 0.70; minor 0.30). Full-matrix least-squares refinement on  $F^2$  based on 5448 independent reflections converged with 341 variable parameters and no restraints.  $R1 = 0.0178$  (for those 5286 data with  $I > 2\sigma(I)$ );  $wR2 = 0.0449$ ; GoF ( $F^2$ ) = 1.033.<sup>[67]</sup>  $\Delta\rho_{\text{max}} = 0.801$  and  $-0.610$  e Å<sup>-3</sup>.

#### Ethylene polymerizations promoted by Nd<sub>x</sub>(OR)<sub>y</sub>/MR<sub>2</sub> combinations prepared in situ:

In a typical experiment, a solution of complex **1** (0.37 g, 0.30 mmol) in toluene (10 mL) was added to a solution of  $\text{Mg}(n\text{-hex})_2$  (0.98 g, 1.0 mmol) in toluene (10 mL) and the reaction mixture was stirred for 1 h at 0 °C. The resulting brown solution was injected through a syringe into a 500 mL Schlenk tube containing toluene (80 mL) kept at 0 °C under 1 atm ethylene (previously saturated solution). Magnetic stirring was started (1100 rpm) and the ethylene consumption was monitored by a mass flowmeter (Aalborg, GFM17) connected to a totalling controller (KEP), which acts as a flow rate integrator. The reaction was quenched by addition of a 5% HCl methanol solution (200 mL) to the reaction mixture and the polymer was recovered by filtration and dried under vacuum.

Experiments conducted at different temperatures, Nd/Mg ratios or in the presence of a transfer agent (feed with a preformed  $\text{C}_2\text{H}_4/\text{H}_2$  mixture or introduction of  $\text{PhSiH}_3$  through a syringe in the reaction mixture after 5 min), and preliminary experiments aimed at evaluating the ability of other lanthanide alkoxide/alkylating reagent combinations, were conducted using a similar procedure.

**Isolation of solid catalyst S:** A typical ethylene polymerization experiment was conducted as described above over 30 min. The resulting reaction mixture was placed under argon and filtrated over a sintering glass funnel while keeping temperature at 0 °C. The clear filtrate was collected under argon at 0 °C for analytical purposes and polymerization catalysis assays. The solid recovered was washed with cold toluene (2 × 50 mL) at 0 °C, to give **S** as a beige gummy solid, which was rapidly used for further polymerization. ICP microanalyses of three different batches of **S** prepared under the above conditions showed that it contains  $15 \pm 2\%$  of Nd and  $20 \pm 4\%$  of Mg initially introduced (as **1** and  $\text{Mg}(n\text{-hex})_2$ , respectively), and the balance for these metals was found in the filtrate. Chlorine content in **S** was below detection limit of elemental analysis.

#### Ethylene polymerizations promoted by isolated solid catalyst S:

*a) Gas phase ethylene polymerization:* The polymerization was carried out directly in the sintering glass funnel by contacting isolated solid **7** with 1 atm of ethylene at 0 °C. In a typical experiment, upon using a solution of **1** (0.37 g, 0.30 mmol) activated by  $\text{Mg}(n\text{-hex})_2$  (0.98 g, 1.0 mmol) in toluene (100 mL) for 1 h at 0 °C allowed to collect, after 10 min of reaction with 1 atm ethylene at 0 °C, 3.4 g **S** as a beige precipitate. The latter was filtered off at 0 °C and washed twice with cold toluene (2 × 50 mL). Ethylene (1 atm) was then contacted onto the beige solid, resulting in the rapid growth of white efflorescence of polyethylene and a consumption of 0.5 g ethylene over 90 min. Upon stirring with a magnetic stir bar in the bottom of the sintering funnel, 1.4 g ethylene were additionally polymerized over 30 min. Quenching and workup as described above afforded 5.4 g polyethylene.

*b) Slurry phase ethylene polymerization:* In a glovebox, freshly prepared solid **S** (typically 4–5 g) was introduced into a 500 mL Schlenk. Cold toluene (100 mL) was introduced and the resulting mixture was placed at 0 °C. After purging with 1 atm ethylene, magnetic stirring was rapidly started (1100 rpm). Ethylene consumption monitoring and final quenching were performed as described above.

**Diblock ethylene-MMA copolymerization:** Diblock ethylene-MMA copolymerization was achieved by reacting a suspension of solid **S** in toluene with MMA at 0 °C. A typical experiment is as follows: Upon using a solution of **1** (0.37 g, 0.30 mmol) activated by Mg(*n*-hex)<sub>2</sub> (0.98 g, 1.0 mmol) in toluene (100 mL) for 1 h at 0 °C allowed to collect, after 10 min of reaction with 1 atm ethylene at 0 °C, **S** (3.3 g) as a beige precipitate. The latter was filtered-off at 0 °C, washed twice with cold toluene (2 × 50 mL) and introduced into a Schlenk-tube with toluene (100 mL) at 0 °C. Freshly distilled MMA (9.0 mL, 90 mmol) was then introduced rapidly (ca. 5 s) through a syringe and the reaction mixture was stirred magnetically (1100 rpm) for 1 h at 0 °C. After addition of a 5% HCl/methanol solution (200 mL), crude polymer was obtained by filtration (4.8 g). Soxhlet extraction with boiling THF for 72 h led to the solubilization of only 3% of the crude material. Most of analytical data for the final copolymer are provided in the text. IR (KBr):  $\tilde{\nu}$  = 1729, 1194, 1148 cm<sup>-1</sup>.

**Reaction of [Nd(O-2,6-*t*Bu<sub>2</sub>-4-Me-C<sub>6</sub>H<sub>2</sub>)<sub>3</sub>] with Mg(*n*-hex)<sub>2</sub>; synthesis of [(*n*-hex)Mg(O-2,6-*t*Bu<sub>2</sub>-4-Me-C<sub>6</sub>H<sub>2</sub>)<sub>2</sub>] (7):** In a glovebox, a solution of [Nd(O-2,6-*t*Bu<sub>2</sub>-4-Me-C<sub>6</sub>H<sub>2</sub>)<sub>3</sub>] (0.42 g, 0.52 mmol) in a minimum of toluene was added to a solution of dry Mg(*n*-hex)<sub>2</sub> (1.01 g, 0.52 mmol) in toluene. The mixture was allowed to stand at -40 °C for three days, resulting in the formation of colourless crystals of **7** that were separated out from the supernatant solution (0.227 g, 90%). <sup>1</sup>H NMR (300 MHz, C<sub>6</sub>D<sub>6</sub>):  $\delta$  = 0.04 (dd,  $J \approx 8$  Hz, 2H, CH<sub>2</sub>Mg), 0.85 (t,  $J = 7.0$  Hz, 3H, CH<sub>3</sub>hex), 1.24 (m, 6H, CH<sub>2</sub>CH<sub>2</sub>CH<sub>2</sub>), 1.54 (s, 6H; *t*Bu), 1.63 (m, 2H; CH<sub>2</sub>), 2.25 (s, 3H; CH<sub>3</sub> Ar), 7.15 (s, 2H; H arom); <sup>13</sup>C NMR (75 MHz, C<sub>6</sub>D<sub>6</sub>):  $\delta$  = 7.6, 14.6, 21.4, 23.3, 29.1, 32.5, 32.9 (CMe<sub>3</sub>), 35.1, 38.2, 127.1, 129.0, 139.4, 154.3; elemental analysis calcd (%) for C<sub>42</sub>H<sub>72</sub>O<sub>2</sub>Mg<sub>2</sub> (657.62): C 76.71, H 11.04; found: C 76.9, H 10.91.

**X-ray crystal structure determination of 7:** A colorless crystal of approximate dimensions 0.29 × 0.32 × 0.46 mm was mounted on a glass fiber. X-ray measurements were made using a Bruker SMART CCD areadetector diffractometer with MoK $\alpha$  ( $\lambda = 0.71073$  Å) at  $T = 163(2)$  K.

Crystal data:<sup>[65]</sup> triclinic  $P\bar{1}$ :  $a = 9.3991(4)$ ,  $b = 9.8064(4)$ ,  $c = 11.5627(5)$  Å;  $\alpha = 92.2830(10)$ ,  $\beta = 106.1100(10)$ ,  $\gamma = 97.9190(10)^\circ$ ;  $V = 1010.72(7)$  Å<sup>3</sup>; formula unit: C<sub>42</sub>H<sub>72</sub>O<sub>2</sub>Mg<sub>2</sub> with  $Z = 1$ ; formula weight: 657.62;  $\rho_{\text{calcd}} = 1.080$  g cm<sup>-3</sup>;  $F(000) = 364$ ;  $\mu(\text{MoK}\alpha) = 0.091$  mm<sup>-1</sup>. 10924 reflections were collected ( $1.84^\circ > \theta > 28.29^\circ$ ). The structure was solved by direct methods.<sup>[66]</sup> The molecule was located about an inversion center. Hydrogen atoms were located from a difference-Fourier map and refined ( $x$ ,  $y$ ,  $z$  and  $U_{\text{iso}}$ ). Full-matrix least-squares refinement on  $F^2$  based on 4783 independent reflections converged with 352 variable parameters and no restraints.  $R1 = 0.0381$  (for those 3952 data with  $I > 2\sigma(I)$ );  $wR2 = 0.1006$ ; GoF ( $F^2$ ) = 1.027.<sup>[67]</sup>  $\Delta\rho_{\text{max}} = 0.365$  and  $-0.189$  e Å<sup>-3</sup>.

**NMR monitoring of 1/MgR<sub>2</sub> combinations:** In a typical experiment, in a glovebox, a Teflon valve NMR tube was charged with **1** (33.6 mg, 0.027 mmol), Mg(*n*-hex)<sub>2</sub>·0.5 heptane (20.0 mg, 0.080 mmol) and 1,2,4,5-tetramethylbenzene (10.6 mg, 0.079 mmol; NMR internal standard). [D<sub>8</sub>]Toluene was then transferred under vacuum at -80 °C, the solution was made homogeneous at this temperature and the tube was introduced in the pre-cooled NMR probe. The progress of the reaction was monitored upon raising the temperature by 10 °C intervals. The formation of 1-hexene ( $\delta$  (<sup>1</sup>H) = 4.98 (m, 2H), 5.72 (m, 1H);  $\delta$  (<sup>13</sup>C) = 108.2, 132.9; confirmed by GC/MS) was observed from -30 °C and that of isobutene ( $\delta$  (<sup>1</sup>H) = 4.70 (s);  $\delta$  (<sup>13</sup>C) = 111.0, 141.7) from 0 °C. After 14 h at 20 °C, the amounts of 1-hexene and isobutene were 40 and 2%, respectively. Resonances for two new Nd species were observed at  $\delta = 23.7$  (relative intensity, 20), 18.5 (10), -5.0 (20), -8.2 (20), -11.1 (10), -69.8 (10) and  $\delta = 25.7$  (2), 19.9 (1), 15.6 (2), 11.3 (1), -6.8 (2), -12.3 (2); other resonances attributable to these species possibly overlapped with signals of diamagnetic species in the range of 4 to -1 ppm.

Reactions performed with [La<sub>3</sub>(OtBu)<sub>9</sub>(thf)<sub>2</sub>] and [Y<sub>3</sub>(OtBu)<sub>9</sub>Cl<sub>2</sub>(thf)<sub>2</sub>] were conducted using a similar protocol.

## Acknowledgement

We gratefully acknowledge Rhodia Electronics & Catalysis for support of this research and for a PhD grant to J.G. We thank Dr. T. Mathivet (Rhodia) for helpful discussions, Prof. R. F. Jordan (University of Chicago) and Mrs. A.-M. Caze, N. Djelal and L. Burylo (University of Lille) for GPC, DSC and XRD measurements.

- [1] For organolanthanide reviews, see: a) H. Schumann, J. A. Meese-Marktscheffel, L. Esser, *Chem. Rev.* **1995**, *95*, 865–986; b) R. Anwänder, W. A. Herrmann, *Top. Curr. Chem.* **1996**, *179*, 1–32; c) F. T. Edelmann, *Top. Curr. Chem.* **1996**, *179*, 247–276; d) R. Anwänder in *Applied Homogeneous Catalysis with Organometallic Compounds, Vol. 2* (Eds: B. Cornils, W. A. Herrmann), Wiley, Weinheim, **1996**, pp. 866–892; e) G. A. Molander, *Chemtracts: Org. Chem.* **1998**, *11*, 237–263; f) R. Anwänder, *Top. Organomet. Chem.* **1999**, *2*, 1–61; g) G. A. Molander, E. C. Dowdy, *Top. Organomet. Chem.* **1999**, *2*, 119–154.
- [2] For leading references, see: a) D. G. H. Ballard, A. Courtis, J. Holton, J. McMeeking, R. Pearce, *Chem. Commun.* **1978**, 994–995; b) P. L. Watson, G. W. Parshall, *Acc. Chem. Res.* **1985**, *18*, 51–56; c) P. L. Watson, T. Herskovitz, *ACS Symp. Ser.* **1983**, *212*, 459–479; d) G. Jeske, H. Lauke, H. Mauermann, P. N. Swepston, H. Schumann, T. J. Marks, *J. Am. Chem. Soc.* **1985**, *107*, 8091–8103; e) G. Jeske, L. E. Schock, P. N. Swepston, H. Schumann, T. J. Marks, *J. Am. Chem. Soc.* **1985**, *107*, 8103–8110; f) B. J. Burger, M. E. Thompson, D. W. Cotter, J. E. Bercaw, *J. Am. Chem. Soc.* **1990**, *112*, 1566–1577; g) M. A. Giardello, Y. Yamamoto, L. Brard, T. J. Marks, *J. Am. Chem. Soc.* **1995**, *117*, 3276–3279; h) H. Yasuda, *Prog. Polym. Sci.* **2000**, *25*, 573–626, and references therein.
- [3] a) G. J. P. Britovsek, V. C. Gibson, D. F. Wass, *Angew. Chem.* **1999**, *111*, 448–468; *Angew. Chem. Int. Ed.* **1999**, *38*, 428–447, and references therein; b) R. F. Jordan, *Adv. Organomet. Chem.* **1991**, *32*, 325–387; c) H. H. Brintzinger, D. Fischer, R. Mulhaupt, B. Rieger, R. M. Waymouth, *Angew. Chem.* **1995**, *107*, 1255–1283; *Angew. Chem. Int. Ed. Engl.* **1995**, *34*, 1143–1170; d) M. Bochmann, *J. Chem. Soc. Dalton Trans.* **1996**, 255–270.
- [4] For reviews on alkoxy and aryloxy chemistry of lanthanides, see: a) K. G. Caulton, L. G. Hubert-Pfalzgraf, *Chem. Rev.* **1990**, *90*, 969–995; b) R. C. Mehrotra, A. Singh, U. M. Tripathi, *Chem. Rev.* **1991**, *91*, 1287–1303; c) L. G. Hubert-Pfalzgraf, *New J. Chem.* **1995**, *19*, 727–750; d) R. Anwänder, *Top. Curr. Chem.* **1996**, *179*, 149–245, and references therein.
- [5] a) C. J. Schaverien, *J. Chem. Soc. Chem. Commun.* **1992**, 11–13; b) C. J. Schaverien, *J. Mol. Catal.* **1994**, *90*, 177–183; c) C. J. Schaverien, *Organometallics* **1994**, *13*, 69–82.
- [6] a) Z. Hou, Y. Zhang, H. Tezuka, P. Xie, O. Tardif, T.-a. Koizumi, H. Yamazaki, Y. Wakatsuki, *J. Am. Chem. Soc.* **2000**, *122*, 10533–10543; b) Z. Hou, S. Kaita, Y. Wakatsuki, *Pure Appl. Chem.* **2001**, *73*, 291–294.
- [7] W. J. Evans, R. N. R. Broomhall-Dillard, J. W. Ziller, *Organometallics* **1996**, *15*, 1351–1355.
- [8] W. J. Evans, J. L. Shreeve, R. N. R. Broomhall-Dillard, J. W. Ziller, *J. Organomet. Chem.* **1995**, *501*, 7–11.
- [9] W. J. Evans, R. N. R. Broomhall-Dillard, J. W. Ziller, *J. Organomet. Chem.* **1998**, *569*, 89–97.
- [10] W. J. Evans, T. J. Boyle, J. W. Ziller, *J. Organomet. Chem.* **1993**, *462*, 141–148.
- [11] W. J. Evans, T. J. Boyle, J. W. Ziller, *J. Am. Chem. Soc.* **1993**, *115*, 5084–5092.
- [12] P. Biagini, G. Lugli, L. Abis, R. Millini, *J. Organomet. Chem.* **1994**, *474*, C16–C18.
- [13] J. C. Gordon, G. R. Giesbrecht, J. T. Brady, D. L. Clark, D. W. Keogh, B. L. Scott, J. G. Watkin, *Organometallics* **2002**, *21*, 127–131.
- [14] P. B. Hitchcock, M. F. Lappert, R. G. Smith, R. A. Bartlett, P. P. Power, *J. Chem. Soc. Chem. Commun.* **1988**, 1007–1009.
- [15] D. L. Clark, J. C. Gordon, J. C. Huffman, J. G. Watkin, B. D. Zwick, *Organometallics* **1994**, *13*, 4266–4270.
- [16] C. J. Schaverien, N. Meijboom, A. G. Orpen, *J. Chem. Soc. Chem. Commun.* **1992**, 124–126.
- [17] Rating of the effectiveness of catalysts for ethylene polymerization is based on Gibson's scale,<sup>[3a]</sup> ranging from very low (activity < 1 gmmol<sup>-1</sup>h<sup>-1</sup>bar<sup>-1</sup>), moderate (activity = 10–100 gmmol<sup>-1</sup>h<sup>-1</sup>bar<sup>-1</sup>), to very high (activity > 1000 gmmol<sup>-1</sup>h<sup>-1</sup>bar<sup>-1</sup>).
- [18] Ethylene polymerization studies with Cp-free group III and lanthanide systems bearing ancillary ligands other than alkoxides have also been conducted, showing very low to high polymerization activity: Tris(pyrazolyl)borate Y and Ln complexes gave moderate activity: a) D. P. Long, P. A. Bianconi, *J. Am. Chem. Soc.* **1996**, *118*, 12453–12454; some benzamidinate and bis(silylamido)biphenyl Y complexes



- have shown very low activity: b) R. Duchateau, C. T. van Wee, A. Meetsma, J. H. Teuben, *J. Am. Chem. Soc.* **1993**, *115*, 4931–4932; c) R. Duchateau, C. T. van Wee, J. H. Teuben, *Organometallics* **1996**, *15*, 2291–2302; d) T. I. Gountchev, T. D. Tilley, *Organometallics* **1999**, *18*, 2896–2905; Sc complexes containing amide-diphosphane and triaza ligands are capable of polymerizing ethylene, although no activity data were reported: e) M. D. Fryzuk, G. Giesbrecht, S. J. Rettig, *Organometallics* **1996**, *15*, 3329–3336; f) S. Hajela, W. P. Schaefer, J. E. Bercaw, *J. Organomet. Chem.* **1997**, *532*, 45–53; cationic alkyl-triaza(monoamido)yttrium complexes have shown high ethylene polymerization activity: g) S. Bambirra, D. van Leusen, A. Meetsma, B. Hessen, J. H. Teuben, *Chem. Commun.* **2001**, 637–638.
- [19] The in situ combination of Al(*i*Bu)<sub>3</sub> with a calix[8]arene neodymium complex (Al/Nd = 15), prepared by reacting calix[8]arene with sodium in a mixture of benzene and 2-propanol and then with NdCl<sub>3</sub>, has been briefly reported to be slowly active in the polymerization of ethylene (2 kg mol<sup>-1</sup> h<sup>-1</sup> bar<sup>-1</sup> at 80 °C over 0.5 h): Z.-Q. Shen, Y.-F. Chen, Y.-F. Zhang, R.-Q. Kou, L.-S. Chen, *Eur. Polym. J.* **2001**, *37*, 1181–1184.
- [20] a) X. Olonde, A. Mortreux, F. Petit, K. Bujadoux, *J. Mol. Catal.* **1993**, *82*, 75–82; b) patent WO 93/07180A1 to ECP Enichem Polymères France [*Chem. Abstr.* **1993**, *119*, 271958s]; c) J.-F. Pelletier, A. Mortreux, F. Petit, X. Olonde, K. Bujadoux, *Stud. Surf. Sci. Catal.* **1994**, *89*, 249–258; d) J.-F. Pelletier, A. Mortreux, X. Olonde, K. Bujadoux, *Angew. Chem.* **1996**, *108*, 1980–1982; *Angew. Chem. Int. Ed. Engl.* **1996**, *35*, 1854–1856; e) S. Bogaert, J.-F. Carpentier, T. Chenal, A. Mortreux, G. Ricart, *Macromol. Chem. Phys.* **2000**, *201*, 1813–1822; f) S. Bogaert, T. Chenal, A. Mortreux, G. Nowogrocki, C. W. Lehmann, J.-F. Carpentier, *Organometallics* **2001**, *20*, 199–205.
- [21] a) W. J. Evans, M. S. Sollberger, T. P. Hanusa, *J. Am. Chem. Soc.* **1988**, *110*, 1841–1850; b) W. J. Evans, M. S. Sollberger, *Inorg. Chem.* **1988**, *27*, 4417–4423; c) W. J. Evans, J. M. Olofson, J. W. Ziller, *Inorg. Chem.* **1989**, *28*, 4309–4311; d) W. J. Evans, J. M. Olofson, J. W. Ziller, *J. Am. Chem. Soc.* **1990**, *112*, 2308–2314; e) W. J. Evans, R. E. Golden, J. W. Ziller, *Inorg. Chem.* **1991**, *30*, 4963–4968.
- [22] a) O. Poncelet, L. G. Hubert-Pfalzgraf, J.-C. Daran, R. Astier, *J. Chem. Soc. Chem. Commun.* **1989**, 1846–1847; b) S. Daniele, L. G. Hubert-Pfalzgraf, P. B. Hitchcock, M. F. Lappert, *Inorg. Chem. Commun.* **2000**, *3*, 218–220.
- [23] a) D. C. Bradley, H. Chudzynska, M. B. Hursthouse, M. Motevalli, *Polyhedron* **1991**, *10*, 1049–1059; b) D. C. Bradley, H. Chudzynska, M. B. Hursthouse, M. Motevalli, *Polyhedron* **1993**, *12*, 1907–1918; c) D. C. Bradley, H. Chudzynska, M. B. Hursthouse, M. Motevalli, *Polyhedron* **1994**, *13*, 7–14.
- [24] D. M. Barnhart, D. L. Clark, J. C. Gordon, J. C. Huffman, J. G. Watkin, B. D. Zwick, *J. Am. Chem. Soc.* **1993**, *115*, 8461–8462.
- [25] R. Anwander, F. C. Munck, T. Priermeier, W. Scherer, O. Runte, W. A. Herrmann, *Inorg. Chem.* **1997**, *36*, 3545–3552.
- [26] G. B. Deacon, B. M. Gatehouse, Q. Shen, G. N. Ward, E. R. T. Tiekink, *Polyhedron* **1993**, *12*, 1289–1294.
- [27] a) M. Wedler, J. W. Gilje, U. Pieper, D. Stalke, M. Noltemeyer, F. T. Edelmann, *Chem. Ber.* **1991**, *124*, 1163–1165; b) F. T. Edelmann, A. Steiner, D. Stalke, J. W. Gilje, S. Jagner, M. Hakansson, *Polyhedron* **1994**, *13*, 539–546.
- [28] a) W. A. Herrmann, R. Anwander, M. Kleine, W. Scherer, *Chem. Ber.* **1992**, *125*, 1971–1979; b) W. A. Herrmann, R. Anwander, W. Scherer, *Chem. Ber.* **1993**, *126*, 1533–1539.
- [29] D. M. Barnhart, D. L. Clark, J. C. Huffman, R. L. Vincent, J. G. Watkin, *Inorg. Chem.* **1993**, *32*, 4077–4083.
- [30] P. B. Hitchcock, M. F. Lappert, I. A. MacKinnon, *J. Chem. Soc. Chem. Commun.* **1988**, 1557–1558.
- [31] J. Gromada, T. Chenal, A. Mortreux, J. W. Ziller, F. Leising, J.-F. Carpentier, *Chem. Commun.* **2000**, 2183–2184.
- [32] M. F. Lappert, A. Singh, R. G. Smith, *Inorg. Synth.* **1990**, *27*, 164–168.
- [33] Aware of the importance of minor details on the outcome of the reactions in this area, special attention has been paid in this study to the reproducibility of the syntheses. Also, it is often questionable how a particular crystal chosen for a single-crystal structure determination is indeed representative of the bulk sample. To address this issue, and given the final objectives of our research, we have checked that isolated crystals and initial bulk materials feature comparable catalytic behavior for olefin polymerization.
- [34] Due to the paramagnetic Nd centers, the <sup>1</sup>H NMR spectra of **1** proved highly temperature sensitive and optimal resolution (minimal resonances overlapping, line shape) was observed at 5 °C.
- [35] Recrystallized samples prepared by salt metathesis using KO*t*Bu (**1**) or by alcoholysis of the Nd amide (**2**) showed invariably more complex <sup>1</sup>H NMR spectra. These spectra ([D<sub>8</sub>]toluene, 5 °C) featured reproducibly as the major (ca. 70%) peaks the seven resonances observed for samples of **1** prepared from Na*t*Bu along with additional (ca. 30%) rather broad resonances (see Experimental Section).
- [36] M. L. Brown, K. S. Mazdiyasi, *Inorg. Chem.* **1970**, *9*, 2783–2786.
- [37] [La<sub>3</sub>(*t*Bu)<sub>9</sub>(thf)<sub>2</sub>], prepared by salt metathesis from LaCl<sub>3</sub> and Na*t*Bu in THF, has been suggested also to be isostructural to **1** on the basis of NMR data.<sup>[21a]</sup> Not surprisingly, Nd-alkoxide chemistry proved much more related to La than Y chemistry.
- [38] C. Wenqi, J. Zhongsheng, X. Yan, F. Yuguo, Y. Guangdi, *Inorg. Chim. Acta* **1987**, *130*, 125–129.
- [39] F. Benetollo, G. Bombieri, C. Bisi Castellani, W. Jahn, R. D. Fischer, *Inorg. Chim. Acta* **1984**, *95*, L7-L10.
- [40] C. W. Decock, S. R. Ely, T. E. Hopkins, M. A. Brault, *Inorg. Chem.* **1978**, *17*, 625–631.
- [41] The THF resonances could not distinguished unambiguously from those of some *t*BuO groups, considering the similar integral ratio, that is 8H vs. 9H, and the experimental uncertainty due to variable line shape.
- [42] L. G. Hubert-Pfalzgraf, S. Daniele, A. Bennaceur, J.-C. Daran, J. Vaissermann, *Polyhedron* **1997**, *16*, 1223–1234.
- [43] a) The synthesis of [LnNa<sub>8</sub>(*t*Bu)<sub>10</sub>Cl] complexes (Ln = Y, Eu) has been reported: W. J. Evans, M. S. Sollenberger, J. W. Ziller, *J. Am. Chem. Soc.* **1993**, *115*, 4120–4127; b) synthesis of [Li<sub>2</sub>Sm(*t*Bu)<sub>8</sub>]: H. Schumann, G. Kociok-Koehn, A. Dietrich, F. H. Goerlitz, *Z. Naturforsch. B: Chem. Sci.* **1991**, *46*, 896–900.
- [44] R. A. Andersen, D. H. Templeton, A. Zalkin, *Inorg. Chem.* **1978**, *17*, 1962–1964.
- [45] a) O. Poncelet, W. J. Sartain, L. G. Hubert-Pfalzgraf, K. Folting, K. G. Caulton, *Inorg. Chem.* **1989**, *28*, 263–267; b) G. Helgesson, S. Jagner, O. Poncelet, L. G. Hubert-Pfalzgraf, *Polyhedron* **1991**, *10*, 1559–1564.
- [46] a) D. C. Bradley, H. Chudzynska, D. M. Frigo, M. B. Hursthouse, M. A. Mazid, *J. Chem. Soc. Chem. Commun.* **1988**, 1258–1259; b) D. C. Bradley, H. Chudzynska, D. M. Frigo, M. E. Hammond, M. B. Hursthouse, M. A. Mazid, *Polyhedron* **1990**, *9*, 719–726.
- [47] M. Kritikos, M. Moustiakimov, M. Wijk, G. Westin, *J. Chem. Soc. Dalton Trans.* **2001**, 1931–1938.
- [48] When the aminolysis reaction was performed in THF, an oily residue was recovered after removal of the volatiles under vacuum. Attempts to extract or to recrystallize this residue were unsuccessful.
- [49] a) R. D. Shannon, C. T. Prewitt, *Acta Crystallogr. Sect. B* **1969**, *25*, 925–946; b) R. D. Shannon, *Acta Crystallogr. Sect. B* **1970**, *26*, 1046–1048; c) R. D. Shannon, *Acta Crystallogr. Sect. A* **1976**, *32*, 751–767.
- [50] Deviation from a Nd/Mg ratio of 1.0, in particular use of an excess of MgR<sub>2</sub> to take into account the presence of two *t*BuOH ligands in **4**, and/or modification of the alkoxy/alkyl metathesis conditions (temperature and time) did not bring any significant improvement of the ethylene polymerization activity of these in situ systems.
- [51] Ethylene polymerization proceeds with (Tp<sup>Me</sup>)YR<sub>2</sub> complexes having two coordinated thf molecules but is inhibited in THF solution; dissociation of coordinated thf from yttrium significantly affects the steric saturation at the metal center and appears to be a controlling factor in the initiation of these polymerizations. See ref. [18a].
- [52] The inefficiency of **3**/Mg(*n*-hex)<sub>2</sub> combinations to promote ethylene polymerization may be related to the presence of chloro bridges in precursor **3** and to the inhibiting effect of NaCl onto the **1**/Mg(*n*-hex)<sub>2</sub> combination. However, the sole presence of chloro ligands in the alkoxy-lanthanide precursor does not preclude the formation of active systems; see ref. [53].
- [53] Ethylene polymerizations (toluene, 0 °C, 1 atm, 1 h using in situ combinations of Mg(*n*-hex)<sub>2</sub> and other lanthanide *tert*-butoxides (Mg/Ln = 1.0) showed lower activities and gave low molecular weight polymers and/or oligomers: “Sm<sub>3</sub>(*t*Bu)<sub>9</sub>(thf)<sub>2</sub>” (this compound was prepared by salt metathesis between SmCl<sub>3</sub> and Na*t*Bu in THF and is supposed to be isostructural to **1** on the basis of <sup>1</sup>H NMR data; see also note [37] and ref. [21a]), *A* = 1.65 kg mol(Sm)<sup>-1</sup> h<sup>-1</sup> bar<sup>-1</sup>, *T*<sub>m</sub> (final PE) = 139 °C, PE recovered after 5 min had *M*<sub>n</sub> = 2500 and *M*<sub>w</sub>/*M*<sub>n</sub> of

- 6.1;  $[\text{La}_3(\text{OtBu})_9(\text{thf})_2]^{[21a]}$   $A = 0.43 \text{ kg mol}(\text{La})^{-1} \text{ h}^{-1} \text{ bar}^{-1}$ ;  $[\text{Y}_3(\text{OtBu})_9\text{Cl}_2(\text{thf})_2]^{[21b]}$   $A = 0.25 \text{ kg mol}(\text{Y})^{-1} \text{ h}^{-1} \text{ bar}^{-1}$ .
- [54]  $^1\text{H}$  ( $\text{C}_2\text{D}_2\text{Cl}_4$ ,  $130^\circ\text{C}$ ):  $\delta = 4.33$  ( $\text{PhSiH}_2$ ),  $0.19$  ( $\text{CH}_2\text{Si}$ );  $^{13}\text{C}$  ( $\text{C}_2\text{D}_2\text{Cl}_4$ ,  $130^\circ\text{C}$ ):  $\delta = 10.0$  ( $\text{CH}_2\text{Si}$ ): P.-F. Fu, T. J. Marks, *J. Am. Chem. Soc.* **1995**, *117*, 10747–10748.
- [55] Similar distribution of the lanthanide metal between the toluene solution and the solid precipitated was observed from the “ $\text{Sm}_3(\text{OtBu})_9(\text{thf})_2$ ”/Mg(*n*-hex)<sub>2</sub>/ethylene system.
- [56] a) Ref. [3]; b) A. D. Horton, J. F. Van Baar, P. A. Schut, G. M. M. Van Kessel, K. L. Von Hebel, *PCT Int. Appl.* WO 9921899 [*Chem. Abs.* **1999**, *130*, 325493]; c) J. A. Ewen, M. J. Elder, *Eur. Pat. Appl.* EP 426638 [*Chem. Abs.* **1991**, *115*, 136987].
- [57] Atactic PMMA with high molecular weight distribution arises from initiation by alkylmagnesium species; the in situ combination  $1/\text{Mg}(\text{n-hex})_2$  initiates the controlled polymerization of MMA to give syndiotactic-rich PMMA with very narrow molecular weight distribution: J. Gromada, C. Fouga, T. Chenal, A. Mortreux, J.-F. Carpentier, *Macromol. Chem. Phys.* **2002**, *203*, 550–555.
- [58] a) For a recent review on compatibilization of polymer blends, see: C. Koning, M. Van Duin, C. Pagnouille, R. Jerome, *Prog. Polym. Sci.* **1998**, *23*, 707–757; b) G. Desurmont, Guillaume, M. Tanaka, Y. Li, H. Yasuda, T. Tokimitsu, S. Tone, A. Yanagase, *J. Polym. Sci. Part A: Polym. Chem.* **2000**, *38*, 4095–4109.
- [59] Successful isolation of a mixed alkyl/aryloxy magnesium complex from the  $[\text{Nd}(\text{O}-2,6\text{-}i\text{Bu}_2\text{-4-Me-C}_6\text{H}_2)_3]/\text{Mg}(\text{n-hex})_2$  system likely results, at least in part, from the beneficial effect of the bulky aryloxy ligand in crystallizing one of the metathesis products. As pointed out by a referee, the basicity of OR may also considerably affect ligand exchange; see ref. [60] for examples of effective metathesis reactions between alkoxy lanthanide complexes and alkylating agents.
- [60] The reaction of  $\text{Ce}(\text{O}i\text{Pr})_4 \cdot i\text{PrOH}$  with 2 equiv  $\text{MgCp}_2$  led to  $[\text{Cp}_3\text{Ce}(\text{O}i\text{Pr})]$  and  $\text{Mg}(\text{O}i\text{Pr})_2$ : a) A. Greco, S. Cesca, G. Bertolini, *J. Organomet. Chem.* **1976**, *113*, 321–330; for lanthanide-alkoxy/alkyl metathesis reactions involving alkylating agents other than dialkylmagnesiums, see: b) V. A. Shreider, E. P. Turevskaya, N. L. Kozlova, N. Y. Turova, *Inorg. Chim. Acta* **1981**, *53*, L73–L76; c) H. Schumann, W. Genthe, N. Brunks, *Organometallics* **1982**, *1*, 1194–1200; d) A. Gulino, N. Casarin, V. P. Conticello, J. G. Gaudiello, T. J. Marks, *Organometallics* **1988**, *7*, 2360–2364.
- [61] R. Duchateau, T. Tuinstra, E. A. C. Brussee, A. Meetsma, P. T. van Duijnen, J. H. Teuben, *Organometallics* **1997**, *16*, 3511–3522 and references therein.
- [62] a) J. W. Bruno, T. J. Marks, L. R. Morss, *J. Am. Chem. Soc.* **1983**, *105*, 6824–6832; b) J. W. Bruno, H. A. Stecher, L. R. Morss, D. C. Sonnenberger, T. J. Marks, *J. Am. Chem. Soc.* **1986**, *108*, 7275–7280; c) S. P. Nolan, D. Stern, T. J. Marks, *J. Am. Chem. Soc.* **1989**, *111*, 7844–7853.
- [63] a) D. C. Bradley, J. S. Ghotra, F. A. Hart, *J. Chem. Soc. Dalton Trans.* **1973**, 1021–1023; b) R. A. Andersen, D. H. Templeton, A. Zalkin, *Inorg. Chem.* **1978**, *17*, 2317–2319.
- [64] R. A. Andersen, G. Wilkinson, *J. Chem. Soc. Dalton Trans.* **1977**, 809–811.
- [65] CCDC-144860 (**1**·THF), -177096 (**3**·2Et<sub>2</sub>O), -177094 (**5**·2 toluene), -177095 (**6**), -177097 (**7**) contain the supplementary crystallographic data for this paper. These data can be obtained free of charge via [www.ccdc.cam.ac.uk/conts/retrieving.html](http://www.ccdc.cam.ac.uk/conts/retrieving.html) (or from the Cambridge Crystallographic Data Centre, 12 Union Road, Cambridge CB21EZ, UK; fax: (+44) 1223-336-033; or [deposit@ccdc.cam.ac.uk](mailto:deposit@ccdc.cam.ac.uk)).
- [66] a) SMART Software Users Guide, Version 5.0, Bruker Analytical X-Ray Systems, Madison, WI, **1999**; b) SAINT Software Users Guide, Version 6.0, Bruker Analytical X-Ray Systems, Madison, WI, **1999**; c) G. M. Sheldrick, SADABS, Bruker Analytical X-Ray Systems, Madison, WI, **1999**; d) G. M. Sheldrick, SHELXTL Version 5.10, Bruker Analytical X-ray Systems, Madison, WI, **1999**.
- [67]  $R1 = \frac{\sum |F_o| - \sum |F_c|}{\sum |F_o|}$ ;  $wR2 = \frac{[\sum (F_o^2 - F_c^2)^2] / [\sum (F_o^2)^2]}{[\sum (F_o^2 - F_c^2)^2] / (n - p)]^{1/2}}$ ; GoF =  $[\frac{\sum (F_o^2 - F_c^2)^2}{(n - p)}]^{1/2}$  where  $n$  is the number of reflections and  $p$  is the total number of parameters refined.

Received: January 14, 2002 [F3800]